Nuclear Quantum Monte Carlo

Robert B. Wiringa, Physics Division, Argonne National Laboratory

WORK WITH

Joe Carlson, Los Alamos

Victor Flambaum, New South Wales

Laura Marcucci, Pisa

Ken Nollett, Argonne

Muslema Pervin, Argonne

Steve Pieper, Argonne

Rocco Schiavilla, JLab & ODU

WORK NOT POSSIBLE WITHOUT EXTENSIVE COMPUTER RESOURCES

Argonne LCRC (Jazz) & MCS Division (BlueGene/L)

Argonne Leadership Computing Facility (BlueGene/P)

NERSC IBM SP's (Seaborg, Bassi)

UNEDF SciDAC & CNS INCITE

Argonne NATIONAL LABORATORY

Physics Division

Work supported by U.S. Department of Energy, Office of Nuclear Physics

Ab Initio CALCULATIONS OF LIGHT NUCLEI

GOALS

Understand nuclei at the level of elementary interactions between individual nucleons, including

- Binding energies, excitation spectra, relative stability
- Densities, electromagnetic moments, transition amplitudes, cluster-cluster overlaps
- Low-energy NA & AA scattering, astrophysical reactions

REQUIREMENTS

- Two-nucleon potentials that accurately describe elastic NN scattering data
- Consistent multi-nucleon potentials and electroweak current operators
- Precise methods for solving the many-nucleon Schrödinger equation

RESULTS

- Quantum Monte Carlo methods can evaluate realistic Hamiltonians accurate to $\sim$1–2%
- About 100 states calculated for $A \leq 12$ nuclei in good agreement with experiment
- Applications to elastic & ineleastic e, π scattering, $(e, e'p)$, (d, p) reactions, etc.
- ^{5}He = $n\alpha$ scattering and low-energy electroweak astrophysical reactions
- We can explore "fine-tuning" issues in nuclear forces and spectra

OUTLINE

Hamiltonian

Variational Monte Carlo

Green's function Monte Carlo

Binding energy results

Nolen-Schiffer anomaly & ^{8}Be isospin-mixing

Densities and radii

Meson-exchange currents and magnetic moments

$M1$, $E2$, F, GT transitions

NA scattering & astrophysical reactions

Nucleon momentum distributions & $A(e,e'pN)$

Sensitivity of nuclear spectra to forces & hadron masses

HAMILTONIAN

$$H = \sum_i K_i + \sum_{i<j} v_{ij} + \sum_{i<j<k} V_{ijk}$$

$$K_i = K_i^{CI} + K_i^{CSB} \equiv -\frac{\hbar^2}{4}[(\frac{1}{m_p} + \frac{1}{m_n}) + (\frac{1}{m_p} - \frac{1}{m_n})\tau_{zi}]\nabla_i^2$$

Argonne v_{18} (AV18)

$v_{ij} = v_{ij}^{\gamma} + v_{ij}^{\pi} + v_{ij}^{I} + v_{ij}^{S} = \sum_p v_p(r_{ij}) O_{ij}^p$

v_{ij}^{γ}: pp, pn & nn electromagnetic terms

$v_{ij}^{\pi} \sim [Y_\pi(r_{ij})\sigma_i \cdot \sigma_j + T_\pi(r_{ij})S_{ij}] \otimes \tau_i \cdot \tau_j$

$v_{ij}^{I} = \sum_p I^p T_\pi^2(r_{ij}) O_{ij}^p$

$v_{ij}^{S} = \sum_p [P^p + Q^p r + R^p r^2] W(r) O_{ij}^p$

$$\begin{aligned} O_{ij}^p = & [1, \sigma_i \cdot \sigma_j, S_{ij}, \mathbf{L}\cdot\mathbf{S}, \mathbf{L}^2, \mathbf{L}^2(\sigma_i \cdot \sigma_j), (\mathbf{L}\cdot\mathbf{S})^2] \\ & + [1, \sigma_i \cdot \sigma_j, S_{ij}, \mathbf{L}\cdot\mathbf{S}, \mathbf{L}^2, \mathbf{L}^2(\sigma_i \cdot \sigma_j), (\mathbf{L}\cdot\mathbf{S})^2] \otimes \tau_i \cdot \tau_j \\ & + [1, \sigma_i \cdot \sigma_j, S_{ij}, \mathbf{L}\cdot\mathbf{S}] \otimes T_{ij} \\ & + [1, \sigma_i \cdot \sigma_j, S_{ij}, \mathbf{L}\cdot\mathbf{S}] \otimes (\tau_i + \tau_j)_z \end{aligned}$$

$S_{ij} = 3\sigma_i \cdot \hat{r}_{ij} \sigma_j \cdot \hat{r}_{ij} - \sigma_i \cdot \sigma_j \qquad T_{ij} = 3\tau_{iz}\tau_{jz} - \tau_i \cdot \tau_j$

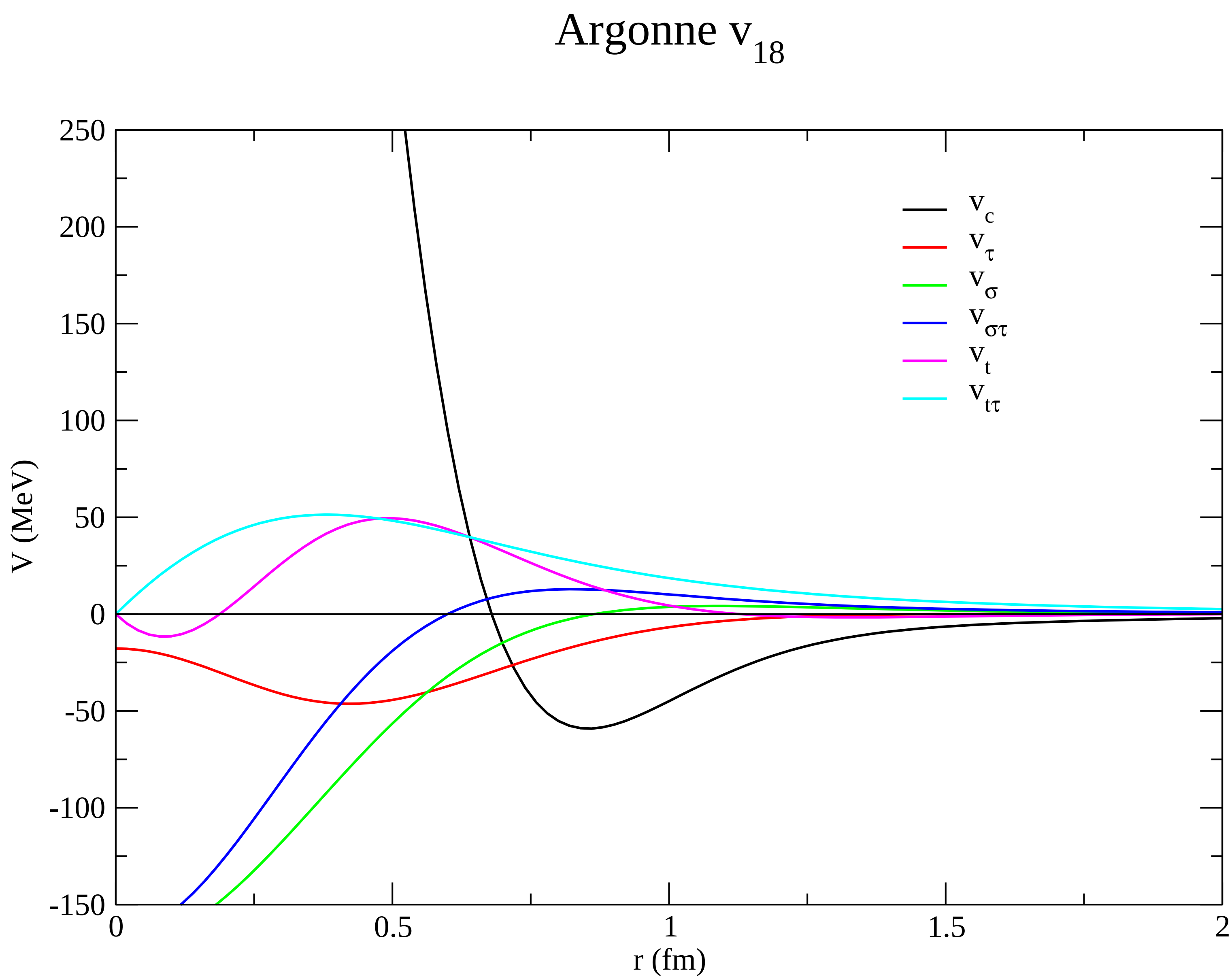

Fits Nijmegen PWA93 data base of 1787 pp & 2514 np observables for $E_{lab} \leq 350$ MeV with χ^2/datum = 1.1 plus nn scattering length and ^{2}H binding energy

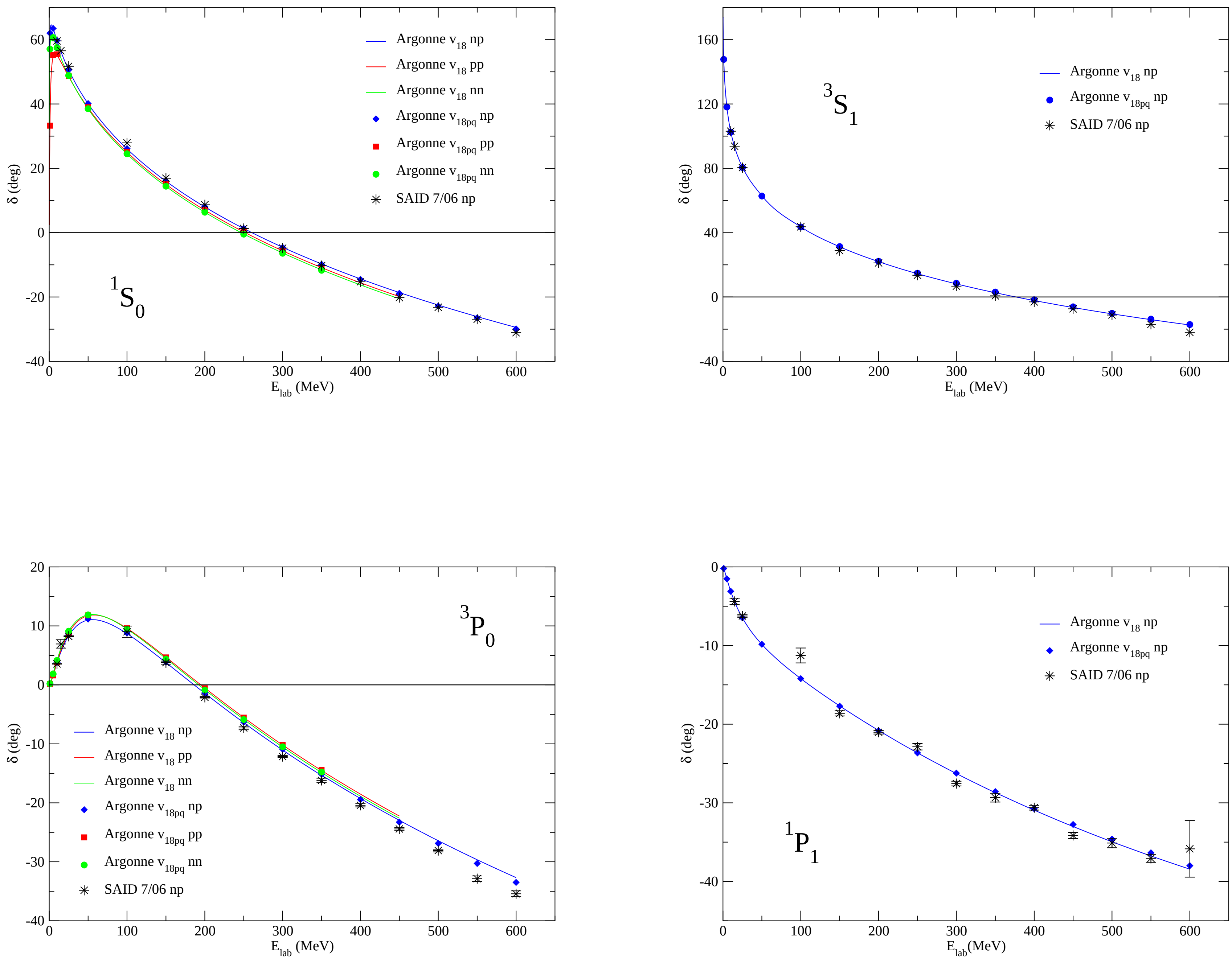

Argonne v18 np
Argonne v18 pp
Argonne v18 nn
Argonne v18pq np
Argonne v18pq pp
Argonne v18pq nn
SAID 7/06 np
1S0
3S1
3P0
1P1
δ (deg)
Elab (MeV)

Three-nucleon potentials

Urbana IX (UIX)

$$V_{ijk} = V_{ijk}^{2\pi P} + V_{ijk}^{R}$$

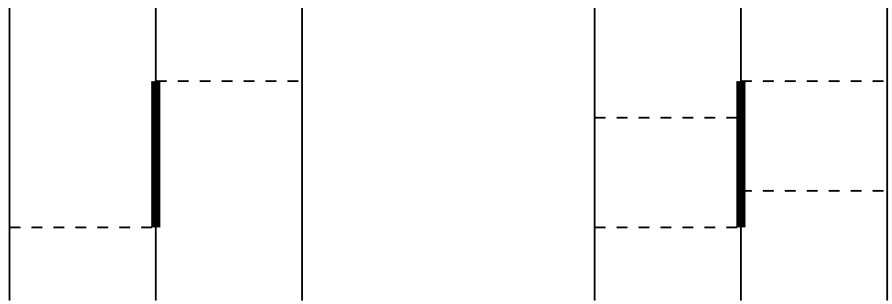

Illinois 2 (IL2,IL7)

$$V_{ijk} = V_{ijk}^{2\pi P} + V_{ijk}^{2\pi S} + V_{ijk}^{3\pi\Delta R} + V_{ijk}^{R}$$

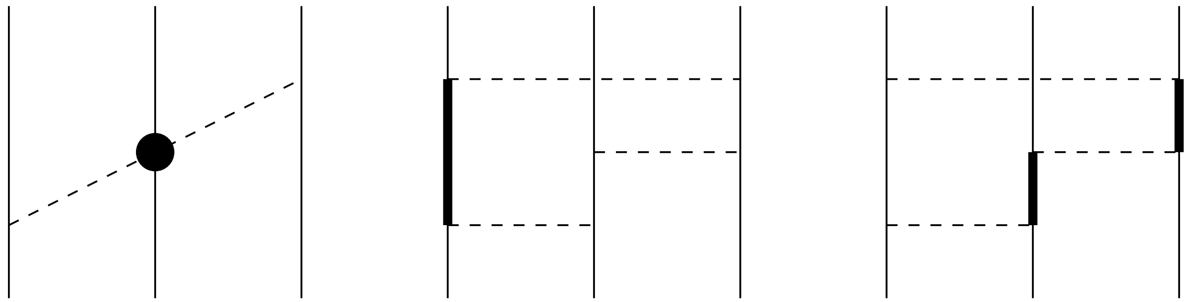

Variational Monte Carlo

Minimize expectation value of H

$$E_V = \frac{\langle \Psi_V | H | \Psi_V \rangle}{\langle \Psi_V | \Psi_V \rangle} \geq E_0$$

Trial function (s-shell nuclei)

$$|\Psi_V\rangle = \left[1 + \sum_{i<j<k} U_{ijk}^{TNI} \right] \left[\mathcal{S} \prod_{i<j} (1 + U_{ij}) \right] |\Psi_J\rangle$$

$$|\Psi_J\rangle = \left[\prod_{i<j} f_c(r_{ij}) \right] |\Phi_A(JMTT_3)\rangle$$

$$|\Phi_d(1100)\rangle = \mathcal{A}| \uparrow p \uparrow n\rangle \;\; ; \;\; |\Phi_\alpha(0000)\rangle = \mathcal{A}| \uparrow p \downarrow p \uparrow n \downarrow n\rangle$$

$$U_{ij} = \sum_{p=2,6} u_p(r_{ij}) O_{ij}^p \;\; ; \;\; U_{ijk}^{TNI} = -\epsilon V_{ijk}(\tilde{r}_{ij}, \tilde{r}_{jk}, \tilde{r}_{ki})$$

Functions $f_c(r_{ij})$ and $u_p(r_{ij})$ obtained from coupled differential equations with v_{ij} .

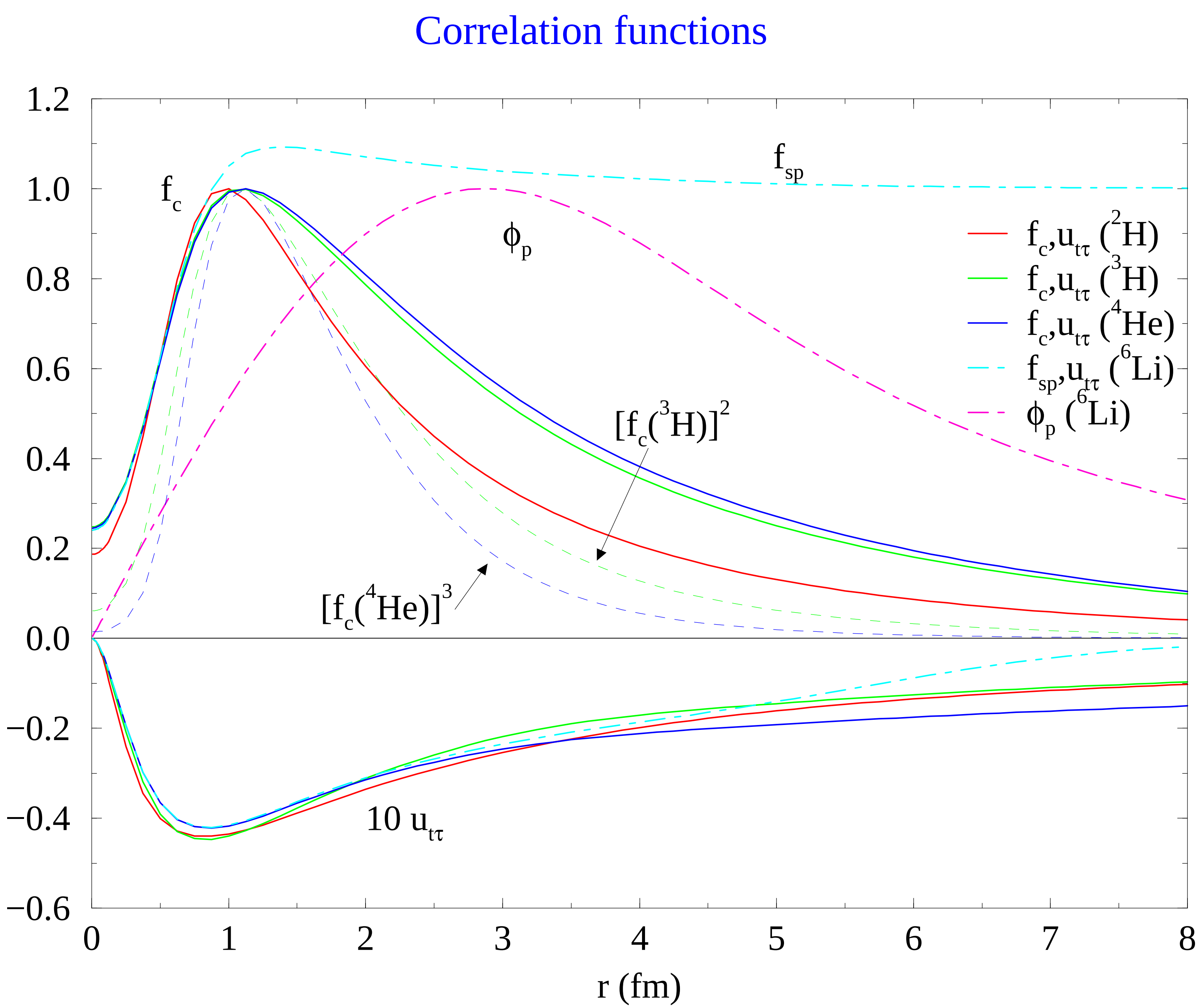
Correlation functions
f_c
f_sp
φ_p
f_c,u_tτ (²H)
f_c,u_tτ (³H)
f_c,u_tτ (⁴He)
f_sp,u_tτ (⁶Li)
φ_p (⁶Li)
[f_c(³H)]²
[f_c(⁴He)]³
10 u_tτ
r (fm)
1.2
1.0
0.8
0.6
0.4
0.2
0.0
−0.2
−0.4
−0.6
0
1
2
3
4
5
6
7
8

Trial function (p-shell nuclei)

$$|\Psi_J\rangle = \mathcal{A}\left\{\prod_{i<j\le 4} f_{ss}(r_{ij}) \sum_{LS[n]} \beta_{LS[n]} \prod_{k\le 4<l\le A} f_{sp}(r_{kl}) \prod_{4<l<m\le A} f_{pp}(r_{lm})\right.$$

$$\left.\Big|\Phi_\alpha(0000)_{1234} \prod_{4<l\le A} \phi_p^{LS[n]}(R_{\alpha l}) \left\{[Y_1^{m_l}(\Omega_{\alpha l})]_{LM_L} \otimes [\chi_l(\tfrac{1}{2}m_s)]_{SM_S}\right\}_{JM} [\nu_l(\tfrac{1}{2}t_3)]_{TT_3}\Big\rangle\right\}$$

Diagonalization

in $\beta_{LS[n]}$ basis to produce energy spectra $E(J^\pi_x)$ and orthogonal excited states $\Psi_V(J^\pi_x)$

Expectation values

$\Psi_V(\mathbf{R})$ represented by vector with $2^A \times \binom{A}{Z}$ spin-isospin components for each space configuration $\mathbf{R} = (\mathbf{r}_1, \mathbf{r}_2, ..., \mathbf{r}_A)$; Expectation values are given by summation over samples drawn from probability distribution $W(\mathbf{R}) = |\Psi_P(\mathbf{R})|^2$:

$$\frac{\langle\Psi_V|O|\Psi_V\rangle}{\langle\Psi_V|\Psi_V\rangle} = \sum \frac{\Psi_V^\dagger(\mathbf{R})O\Psi_V(\mathbf{R})}{W(\mathbf{R})} \Big/ \sum \frac{\Psi_V^\dagger(\mathbf{R})\Psi_V(\mathbf{R})}{W(\mathbf{R})}$$

$\Psi^\dagger\Psi$ is a dot product and $\Psi^\dagger O\Psi$ a sparse matrix operation.

Green's Function Monte Carlo

Projects out lowest energy state from variational trial function

$$\begin{aligned}\Psi(\tau) = \exp[-(H-E_0)\tau]\Psi_V &= \sum_n \exp[-(E_n - E_0)\tau] a_n \psi_n \\ \Psi(\tau \to \infty) &= a_0 \psi_0\end{aligned}$$

Evaluation of $\Psi(\tau)$ done stochastically in small time steps $\Delta\tau$

$$\Psi(\mathbf{R}_n, \tau) = \int G(\mathbf{R}_n, \mathbf{R}_{n-1}) \cdots G(\mathbf{R}_1, \mathbf{R}_0) \Psi_V(\mathbf{R}_0) d\mathbf{R}_{n-1} \cdots d\mathbf{R}_0$$

using the short-time propagator accurate to order $(\Delta\tau)^3$ (V_{ijk} term omitted for simplicity)

$$G_{\alpha\beta}(\mathbf{R}, \mathbf{R}') = e^{E_0 \Delta\tau} G_0(\mathbf{R}, \mathbf{R}') \langle\alpha| \left[\mathcal{S} \prod_{i<j} \frac{g_{ij}(\mathbf{r}_{ij}, \mathbf{r}'_{ij})}{g_{0,ij}(\mathbf{r}_{ij}, \mathbf{r}'_{ij})} \right] |\beta\rangle$$

where the free many-body propagator is

$$G_0(\mathbf{R}, \mathbf{R}') = \langle \mathbf{R} | e^{-K \triangle\tau} | \mathbf{R}' \rangle = \left[\sqrt{\frac{m}{2\pi\hbar^2 \triangle\tau}} \right]^{3A} \exp\left[\frac{-(\mathbf{R}-\mathbf{R}')^2}{2\hbar^2 \triangle\tau / m} \right]$$

and $g_{0,ij}$ and g_{ij} are the free and exact two-body propagators

$$g_{ij}(\mathbf{r}_{ij}, \mathbf{r}'_{ij}) = \langle \mathbf{r}_{ij} | e^{-H_{ij} \triangle\tau} | \mathbf{r}'_{ij} \rangle$$

Mixed estimates

$$\langle O(\tau)\rangle = \frac{\langle\Psi(\tau)|O|\Psi(\tau)\rangle}{\langle\Psi(\tau)|\Psi(\tau)\rangle} \approx \langle O(\tau)\rangle_{\mathrm{Mixed}} + [\langle O(\tau)\rangle_{\mathrm{Mixed}} - \langle O\rangle_V]$$

$$\langle O(\tau)\rangle_{\mathrm{Mixed}} = \frac{\langle\Psi_V|O|\Psi(\tau)\rangle}{\langle\Psi_V|\Psi(\tau)\rangle} \quad ; \quad \langle H(\tau)\rangle_{\mathrm{Mixed}} = \frac{\langle\Psi(\tau/2)|H|\Psi(\tau/2)\rangle}{\langle\Psi(\tau/2)|\Psi(\tau/2)\rangle} \geq E_0$$

Propagator cannot contain p^2, L^2, or $(\mathbf{L}\cdot\mathbf{S})^2$ operators:

$G_{\beta\alpha}(\mathbf{R}',\mathbf{R})$ has only v_8'

$\langle v_{18} - v_8'\rangle$ computed perturbatively with extrapolation (small for AV18)

Fermion sign problem limits maximum τ:

$G_{\beta\alpha}(\mathbf{R}',\mathbf{R})$ brings in lower-energy boson solution

$\langle\Psi_V|H|\Psi(\tau)\rangle$ projects back fermion solution. but statistical errors grow exponentially

Constrained-path propagation, removes steps that have

$$\overline{\Psi^\dagger(\tau,\mathbf{R})\Psi(\mathbf{R})} = 0$$

Possible systematic errors reduced by $10-20$ unconstrained steps before evaluating observables.

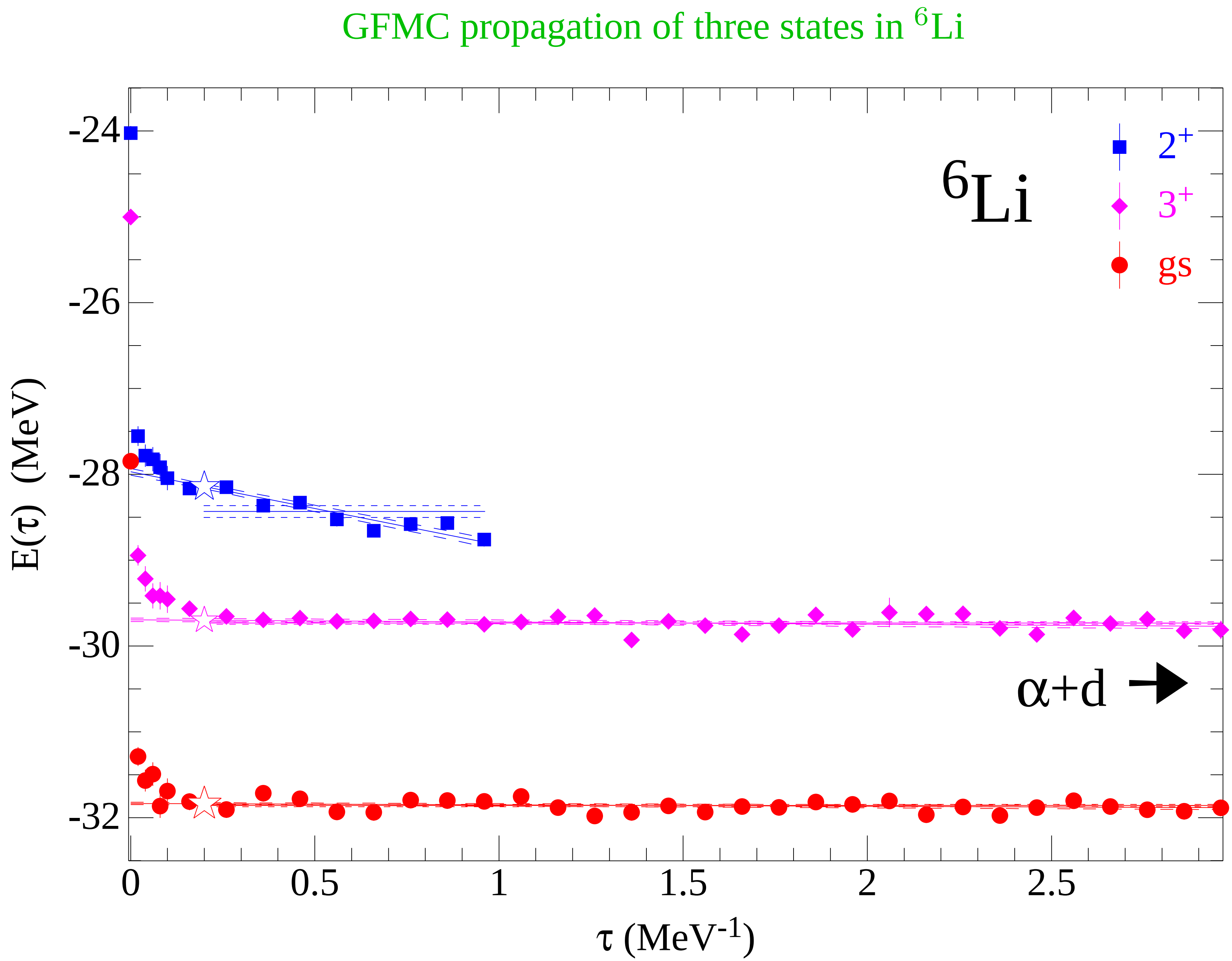
GFMC propagation of three states in ^{6}Li
^{6}Li
2^+
3^+
gs
α+d
-24
-26
-28
-30
-32
0
0.5
1
1.5
2
2.5
E(τ) (MeV)
τ (MeV^{-1})

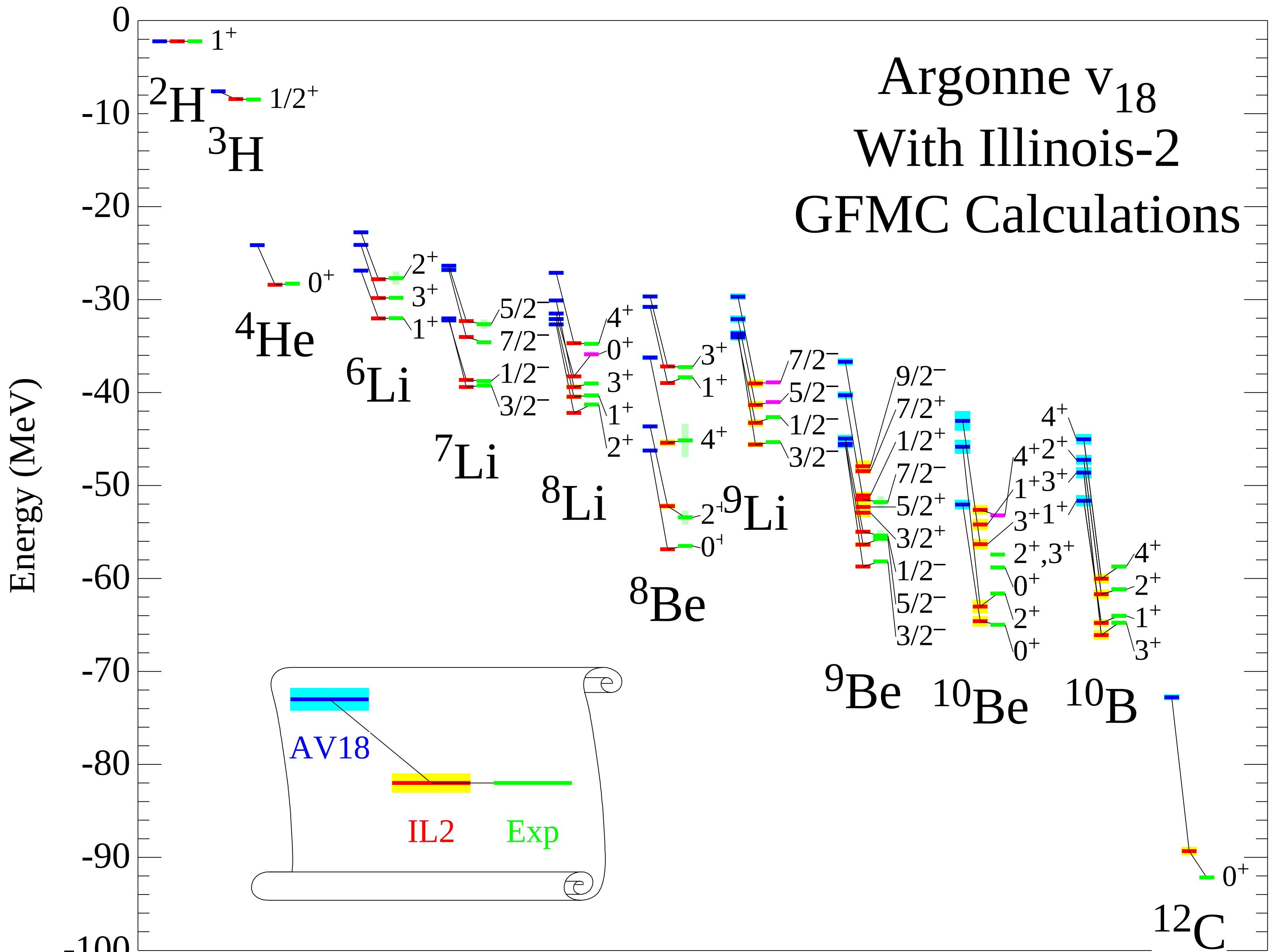

Argonne v18
With Illinois-2
GFMC Calculations
Energy (MeV)
0
-10
-20
-30
-40
-50
-60
-70
-80
-90
-100
2H
3H
4He
6Li
7Li
8Li
8Be
9Li
9Be
10Be
10B
12C
1+
1/2+
0+
2+
3+
1+
5/2−
7/2−
1/2−
3/2−
4+
0+
3+
1+
2+
3+
1+
4+
2+
0+
7/2−
5/2−
1/2−
3/2−
9/2−
7/2+
1/2+
7/2−
5/2+
3/2+
1/2−
5/2−
3/2−
4+
1+
3+
2+,3+
0+
2+
0+
4+
2+
3+
1+
4+
2+
1+
3+
0+
AV18
IL2
Exp

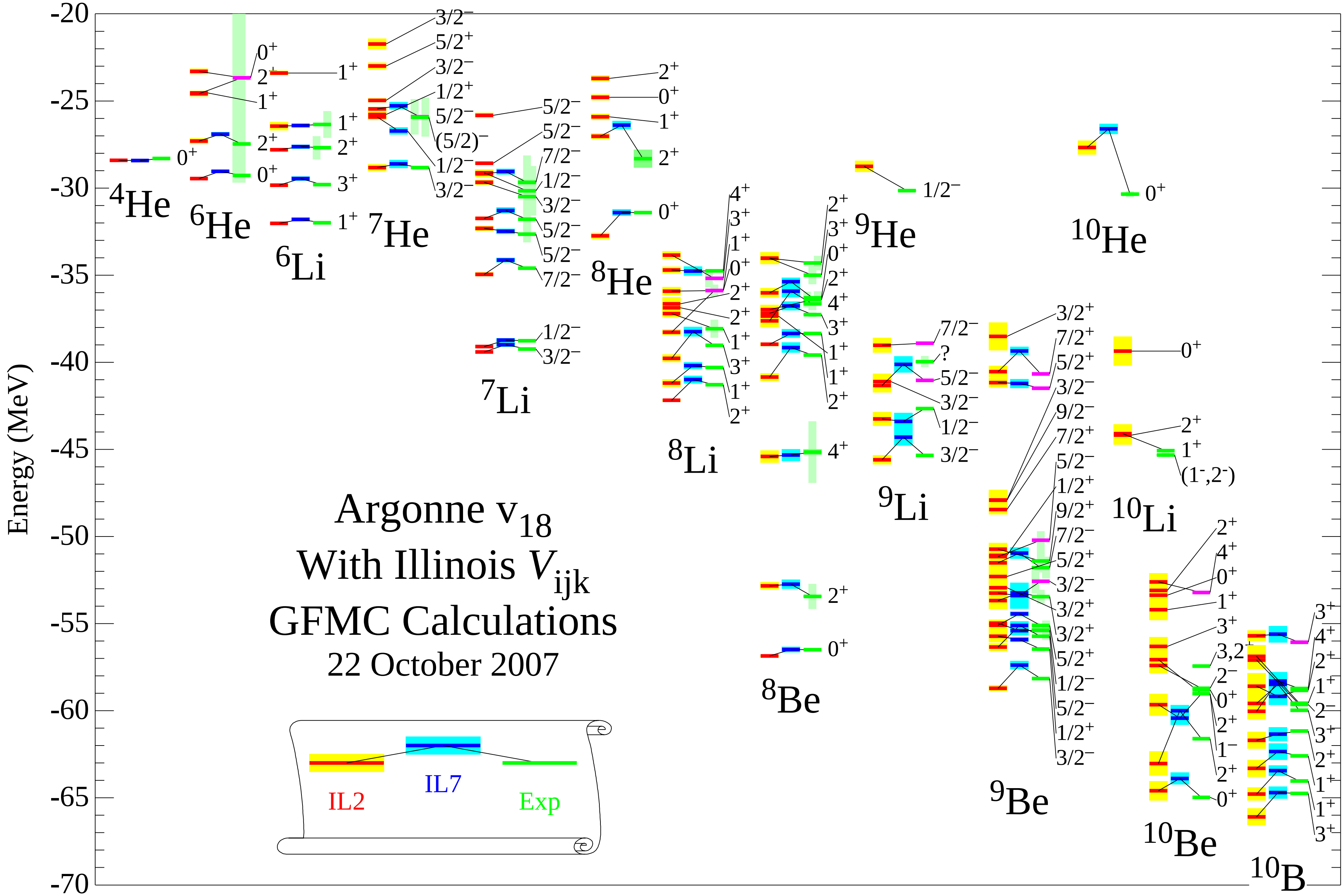

Energy (MeV)
Argonne v_{18}
With Illinois V_{ijk}
GFMC Calculations
22 October 2007
IL2
IL7
Exp
^{4}He
^{6}He
^{6}Li
^{7}He
^{7}Li
^{8}He
^{8}Li
^{8}Be
^{9}He
^{9}Li
^{10}He
^{9}Be
^{10}Li
^{10}Be
^{10}B

Nolen-Schiffer Anomaly

Extract isovector [CSB $\propto (\tau_1 + \tau_2)_z$] & isotensor [CD $\propto T_{12}$] energy components:

$$E_{A,T}(T_z) = \sum_{n \leq 2T} a_n(A,T) Q_n(T,T_z)$$

$Q_0 = 1\,;\, Q_1 = T_z\,;\, Q_2 = \frac{1}{2}(3T_z^2 - T^2)$

Strong Type III CSB (constrained $\pm 20\%$ by nn scattering length) fixes isovector terms.

Strong Type II CD (constrained by $^1S_0$ pp and np scattering) overdoes isotensor; need P-wave NN scattering constraint?

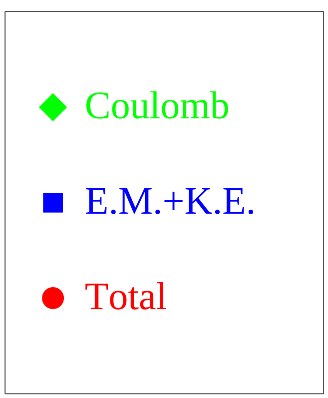

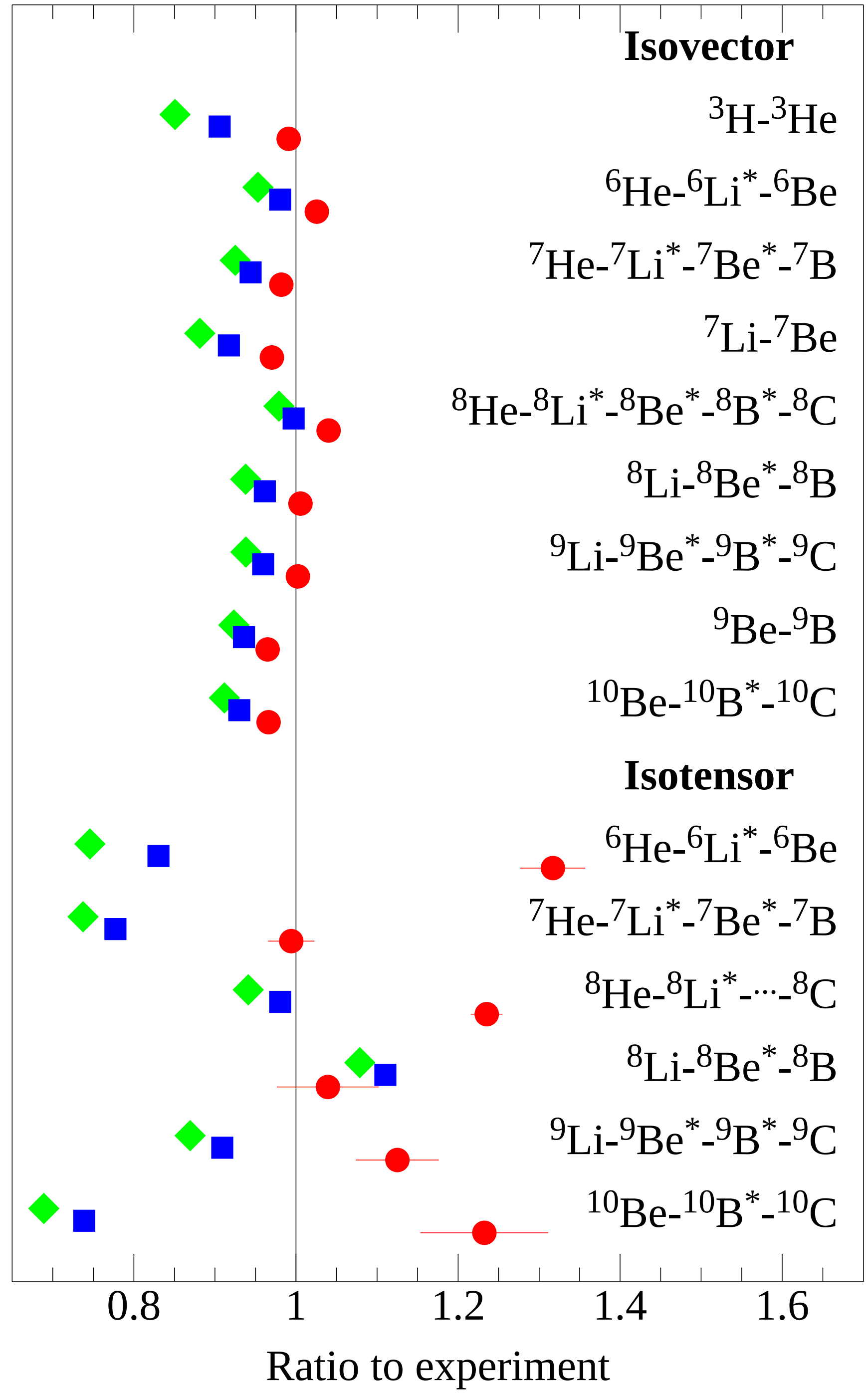

GFMC isovector and isoscalar energy coefficients for AV18+IL7 in keV

$a_n(A,T)$	K^{CSB}	$v_{C1}(pp)$	$v^{\gamma,R}$	v^{CSB}+v^{CD}	Total	Expt.
$a_1(3,\frac{1}{2})$	14	650(0)	28	65(0)	757(0)	764
$a_1(6,1)$	18	1118(2)	14	54(1)	1203(2)	1173
$a_1(7,\frac{1}{2})$	23	1446(3)	36	86(1)	1592(4)	1641
$a_1(7,\frac{3}{2})$	17	1270(3)	9	52(1)	1348(4)	1373
$a_1(8,1)$	23	1660(4)	19	78(1)	1780(5)	1770
$a_1(8,2)$	22	1624(4)	8	71(1)	1726(4)	1659
$a_1(9,\frac{1}{2})$	19	1709(6)	4	55(1)	1786(7)	1851
$a_1(9,\frac{3}{2})$	26	1974(6)	19	90(1)	2109(7)	2104
$a_1(10,1)$	25	2123(7)	18	55(1)	2250(8)	2329
$a_2(6,1)$		167(0)	19	109(8)	295(9)	224
$a_2(7,\frac{3}{2})$		129(0)	7	38(5)	174(5)	175
$a_2(8,1)$		137(1)	4	−10(8)	132(8)	145
$a_2(8,2)$		144(0)	6	39(3)	189(3)	127
$a_2(9,\frac{3}{2})$		153(1)	7	38(8)	198(9)	176
$a_2(10,1)$		166(1)	12	119(18)	297(19)	241

Isospin-mixing in ^{8}Be

Experimental energies of 2^+ states

E_a = 16.626(3) MeV Γ_a^α = 108.1(5) keV

E_b = 16.922(3) MeV Γ_b^α = 74.0(4) keV

Isospin mixing of 2^+;1 and 2^+;0*

states due to isovector interaction H_{01}:

$\Psi_a = \beta\Psi_0 + \gamma\Psi_1$; $\Psi_b = \gamma\Psi_0 - \beta\Psi_1$

decay through $T = 0$ component only

$\Gamma_a^\alpha/\Gamma_b^\alpha = \beta^2/\gamma^2 \Rightarrow \beta = 0.77$; $\gamma = 0.64$

$$E_{a,b} = \frac{H_{00}+H_{11}}{2} \pm \sqrt{\left(\frac{H_{00}-H_{11}}{2}\right)^2 + (H_{01})^2}$$

$H_{00} = 16.746(2)$ MeV

$H_{11} = 16.802(2)$ MeV

$H_{01} = -145(3)$ keV

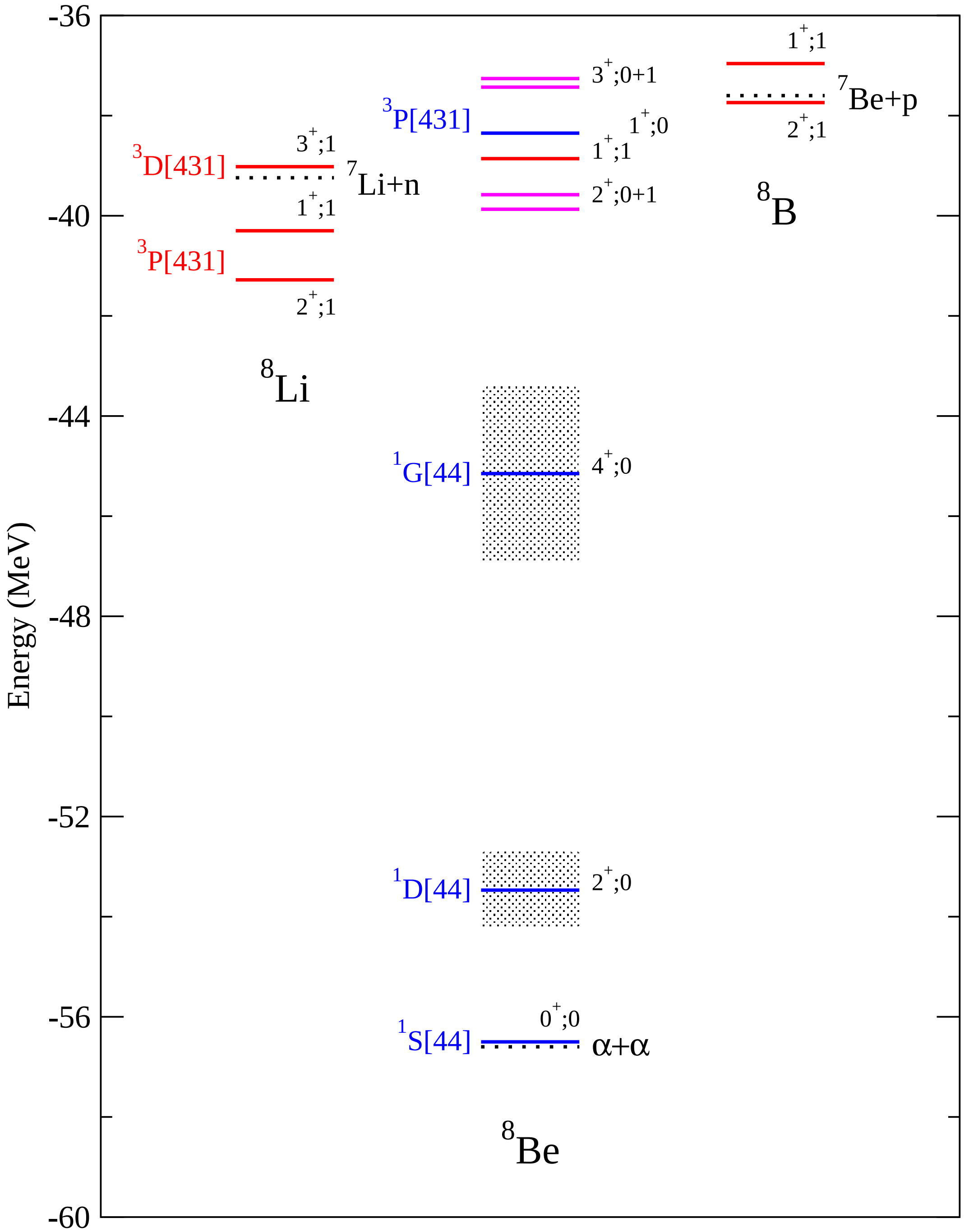

Isospin-mixing matrix elements in keV

		H_{01}	K^{CSB}	V^{CSB}	V_γ	(Coul)	(MM)
$2^+;1 \Leftrightarrow 2^+_2;0$	GFMC	$-115(3)$	$-3.1(2)$	$-21.3(6)$	$-90.3(26)$	$-78.3(25)$	$-12.0(2)$
	Barker	$-145(3)$				-67	
$1^+;1 \Leftrightarrow 1^+;0$	GFMC	$-102(4)$	$-2.9(2)$	$-18.2(6)$	$-80.3(30)$	$-79.5(30)$	$-0.8(2)$
	Barker	$-120(1)$				-54	
$3^+;1 \Leftrightarrow 3^+;0$	GFMC	$-90(3)$	$-2.5(2)$	$-14.8(6)$	$-73.1(21)$	$-60.9(21)$	$-12.2(2)$
	Barker	$-62(15)$				-32	
$2^+;1 \Leftrightarrow 2^+_1;0$	GFMC	$-6(2)$	$-0.4(2)$	$-1.3(4)$	$-4.4(12)$		

Barker, Nucl.Phys. **83**, 418 (1966)

Coulomb terms are about half of H_{01}, but magnetic moment and strong Type III CSB are relatively more important than in Nolen-Schiffer anomaly; still missing $\approx 20\%$ of strength.

Strong Type IV CSB will also contribute (probably best nuclear structure place to look):

$$\begin{aligned} V^{CSB}_{IV} &= (\tau_1 - \tau_2)_z(\sigma_1 - \sigma_2)\cdot\mathbf{L}\, v(r) \\ &+ (\tau_1 \times \tau_2)_z(\sigma_1 \times \sigma_2)\cdot\mathbf{L}\, w(r) \end{aligned}$$

Preliminary result: $v^\gamma \propto \mu_n \sim -2$ keV & $w^\pi \propto (M_n - M_p) \sim -2$ keV.

Single-nucleon densities

$$\rho_{p,n}(r) = \sum_i \langle\Psi|\delta(r-r_i)\frac{1\pm\tau_i}{2}|\Psi\rangle$$

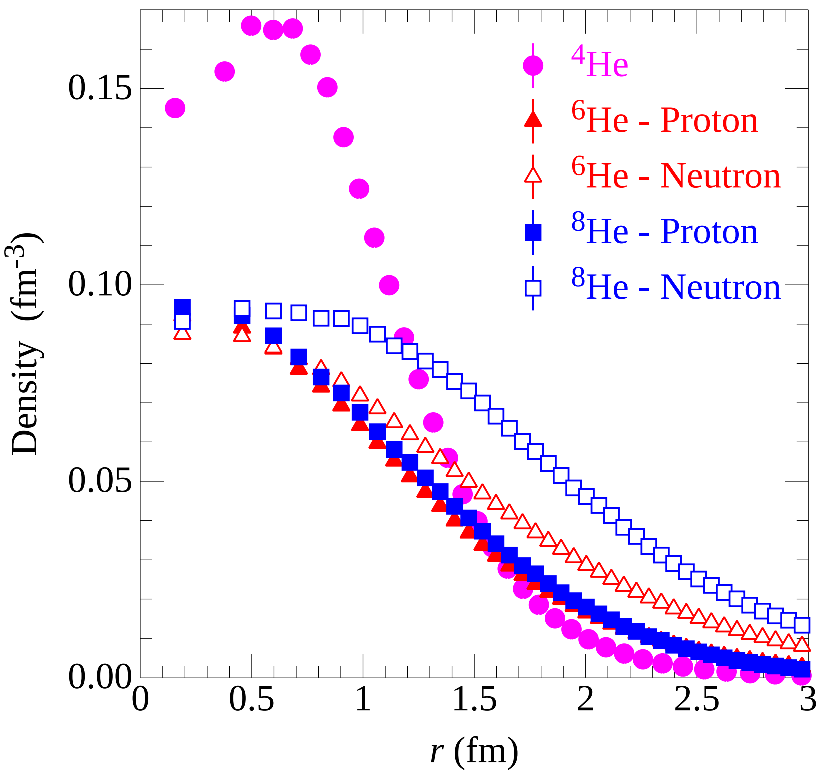

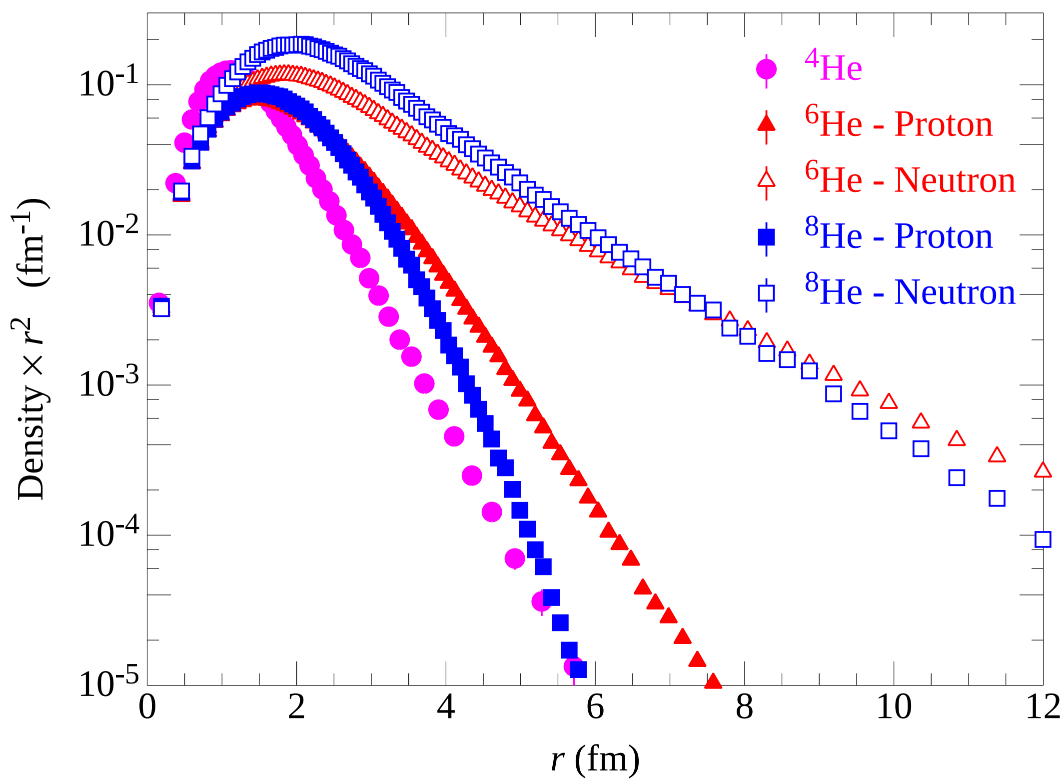

RMS radii

	r_n	r_p	r_c	Expt
^{4}He	1.45(1)	1.45(1)	1.67(1)	1.681(4)*
^{6}He	2.86(6)	1.92(4)	2.06(4)	2.072(9)†
^{8}He	2.79(3)	1.82(2)	1.94(2)	1.961(16)‡

*Sick, PRC **77**, 041302(R) (2008)

†Wang, *et al.*, PRL **93**, 142501 (2004)

‡Mueller, *et al.*, PRL **99**, 252501 (2007)

Two-nucleon densities

$$\rho_{pp}(r) = \sum_{i<j} \langle \Psi | \delta(r - |\mathbf{r}_i - \mathbf{r}_j|) \frac{1+\tau_i}{2} \frac{1+\tau_j}{2} | \Psi \rangle$$

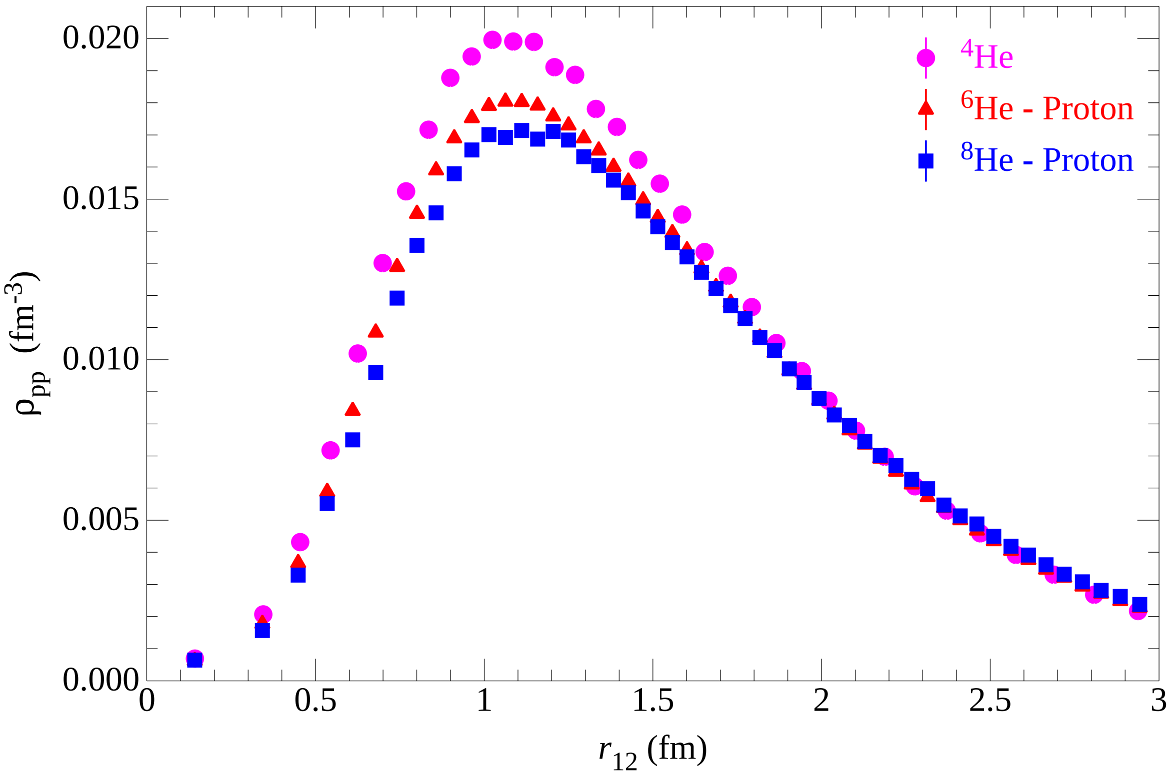

RMS radii

	r_{pp}	r_{np}	r_{nn}
^{4}He	2.41	2.35	2.41
^{6}He	2.51	3.69	4.40
^{8}He	2.52	3.58	4.37

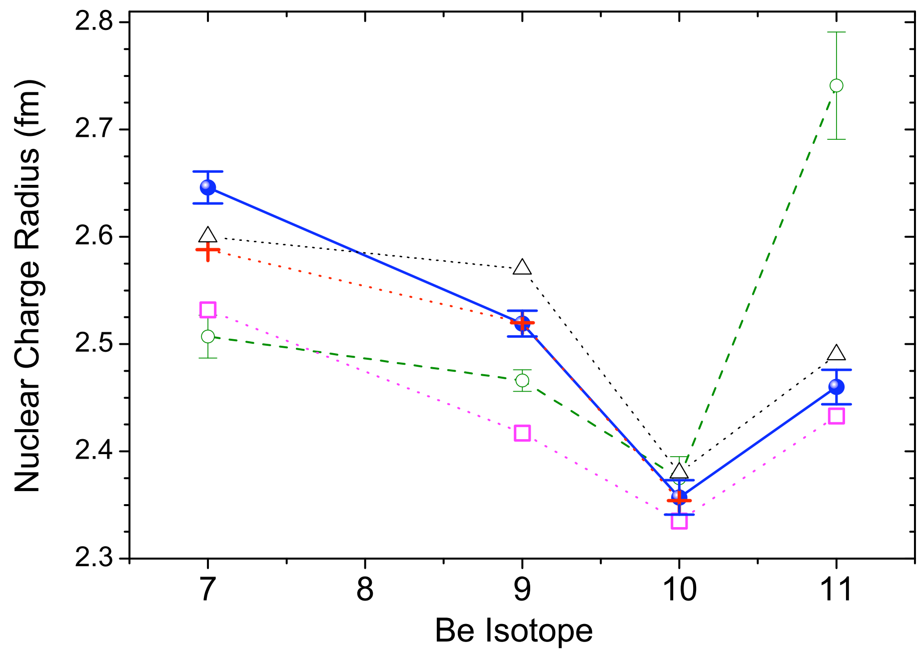

FIG. 3: (Color online) Experimental charge radii of beryllium isotopes from isotope shift measurements (●) compared with values from interaction cross section measurements (○) and theoretical predictions: Greens-Function Monte-Carlo calculations (+) [20, 21], Fermionic Molecular Dynamics (△) [22], *ab-initio* No-Core Shell Model (□) [12, 23, 24].

Nörtershäuser, *et al.*, arXiv:0809.2607

Nuclear Electromagnetic Currents

Marcucci *et al.* (2005)

$$\mathbf{j} = \mathbf{j}^{(1)}$$

$$+\ \mathbf{j}^{(2)}(\mathrm{v}) +$$

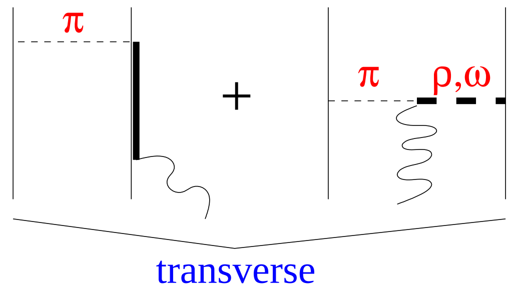

$$+\ \mathbf{j}^{(3)}(\mathrm{V}^{2\pi})$$

- Gauge invariant:

$$\mathbf{q} \cdot \left[\mathbf{j}^{(1)} + \mathbf{j}^{(2)}(v) + \mathbf{j}^{(3)}(V^{2\pi})\right] = \left[T + v + V^{2\pi}\,,\ \rho\right]$$

ρ is the nuclear charge operator

Magnetic Moments

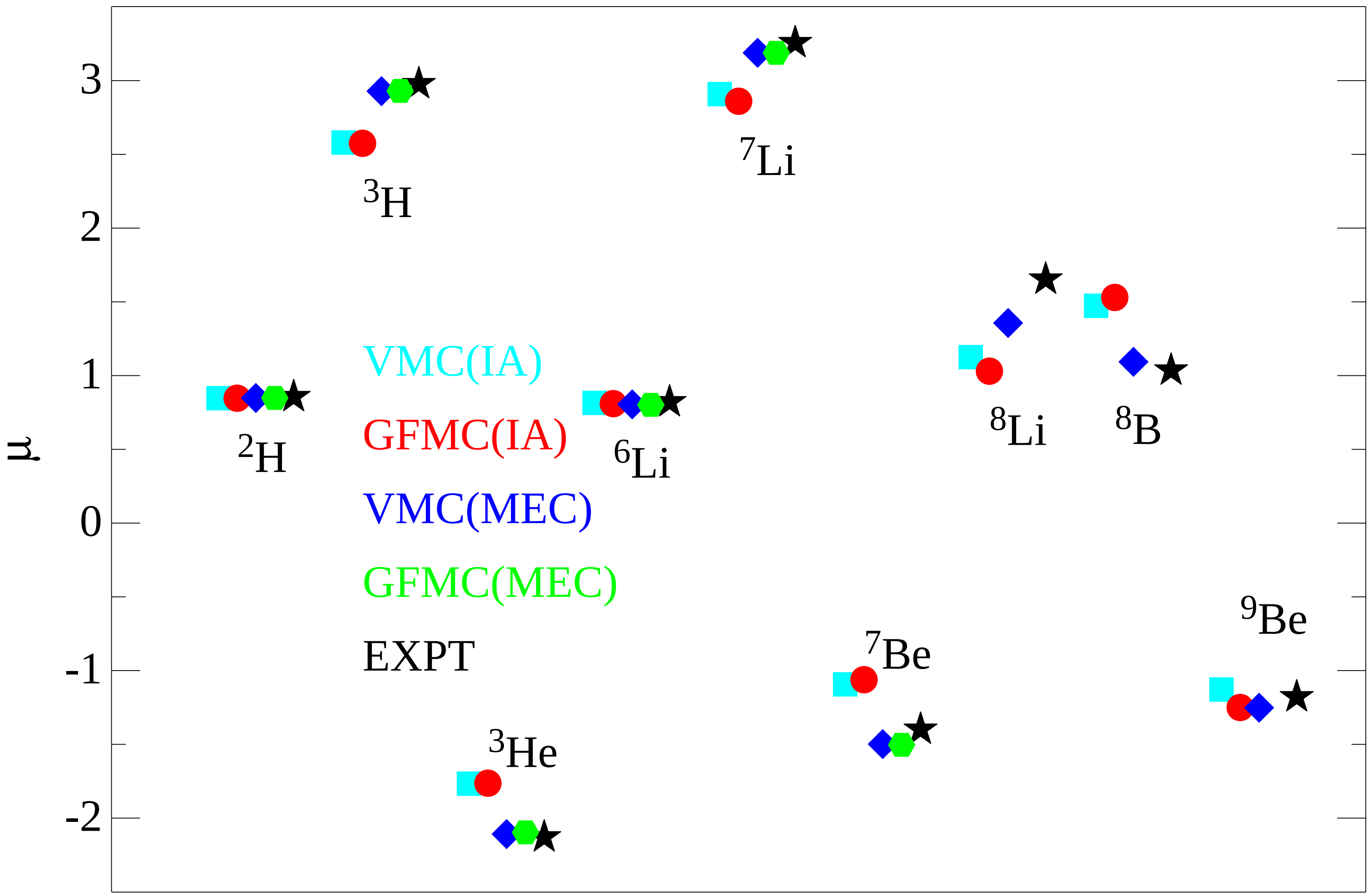

Marcucci, Pervin, *et al.* PRC **78**, 065501 (2008)

$M1$, $E2$, F, GT transitions

$$E2 = e\sum_k \tfrac{1}{2}\left[r_k^2 Y_2(\hat{r}_k)\right](1+\tau_{kz})$$
$$M1 = \mu_N \sum_k [(L_k + g_p S_k)(1+\tau_{kz})/2 + g_n S_k (1-\tau_{kz})/2]$$

$$\mathrm{F} = \sum_k \tau_{k\pm} \;;\; \mathrm{GT} = \sum_k \sigma_k \tau_{k\pm}$$

Pervin, Pieper & Wiringa, PRC **76**, 064319 (2007)

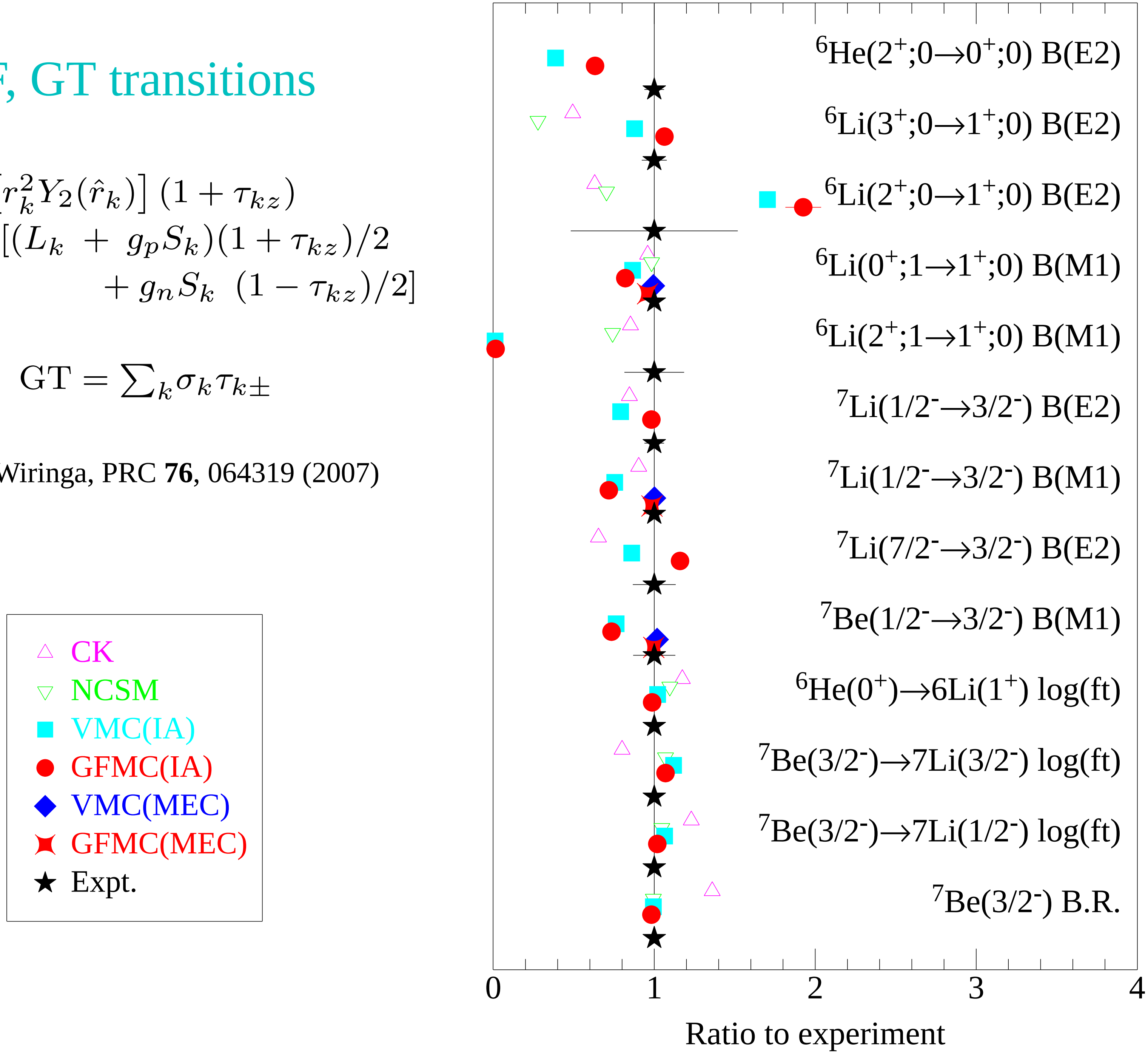

GFMC FOR SCATTERING STATES

GFMC treats nuclei as particle-stable system – should be good for energies of narrow resonances
Need better treatment for locations and widths of wide states and for capture reactions

METHOD

- Pick a logarithmic derivative, χ, at some large boundary radius ($R_B \approx 9$ fm)
- GFMC propagation, using method of images to preserve χ at R, finds $E(R_B, \chi)$
- Phase shift, $\delta(E)$, is function of R_B, χ, E
- Repeat for a number of χ until $\delta(E)$ is mapped out

Example for ^{5}He($\frac{1}{2}^-$)

- "Bound-state" boundary condition does not give stable energy; Decaying to n+^{4}He threshold
- Scattering boundary condition produces stable energy.

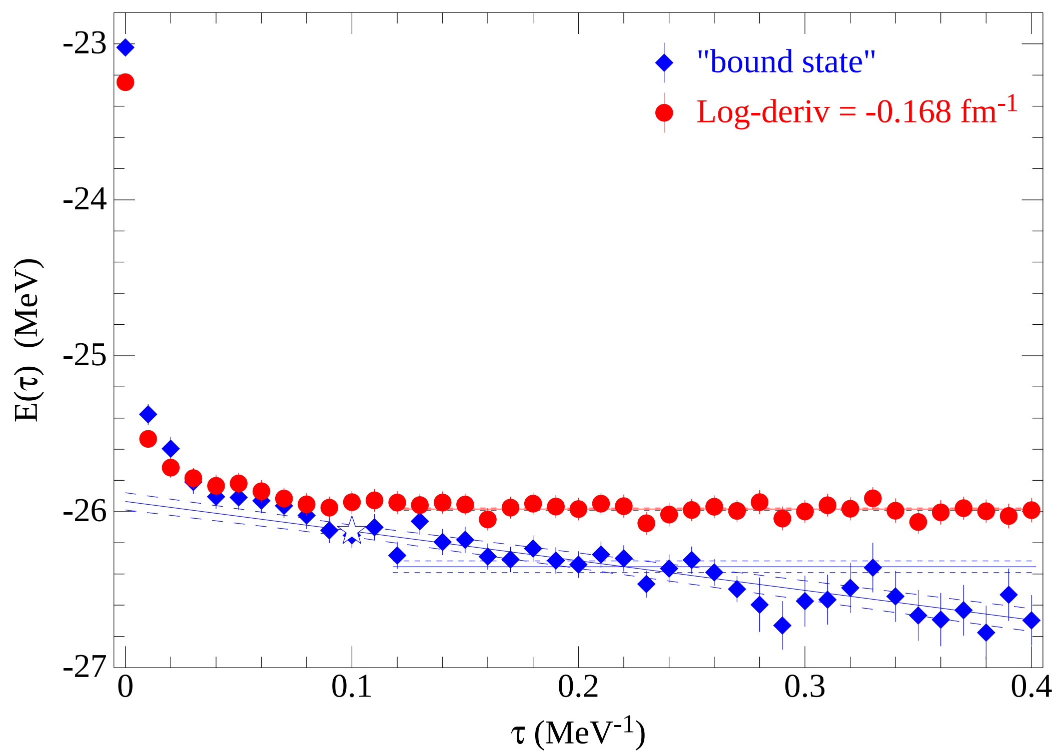

GFMC for ^{5}He as n+^{4}He Scattering States

Black curves: Hale phase shifts from R-matrix analysis up to $J = \frac{9}{2}$ of data

AV18 with no V_{ijk} underbinds ^{5}He($3/2^-$) & overbinds ^{5}He($1/2^-$)

AV18+UIX improves ^{5}He($1/2^-$) but still too small spin-orbit splitting

AV18+IL2 reproduces locations and widths of both P-wave resonances

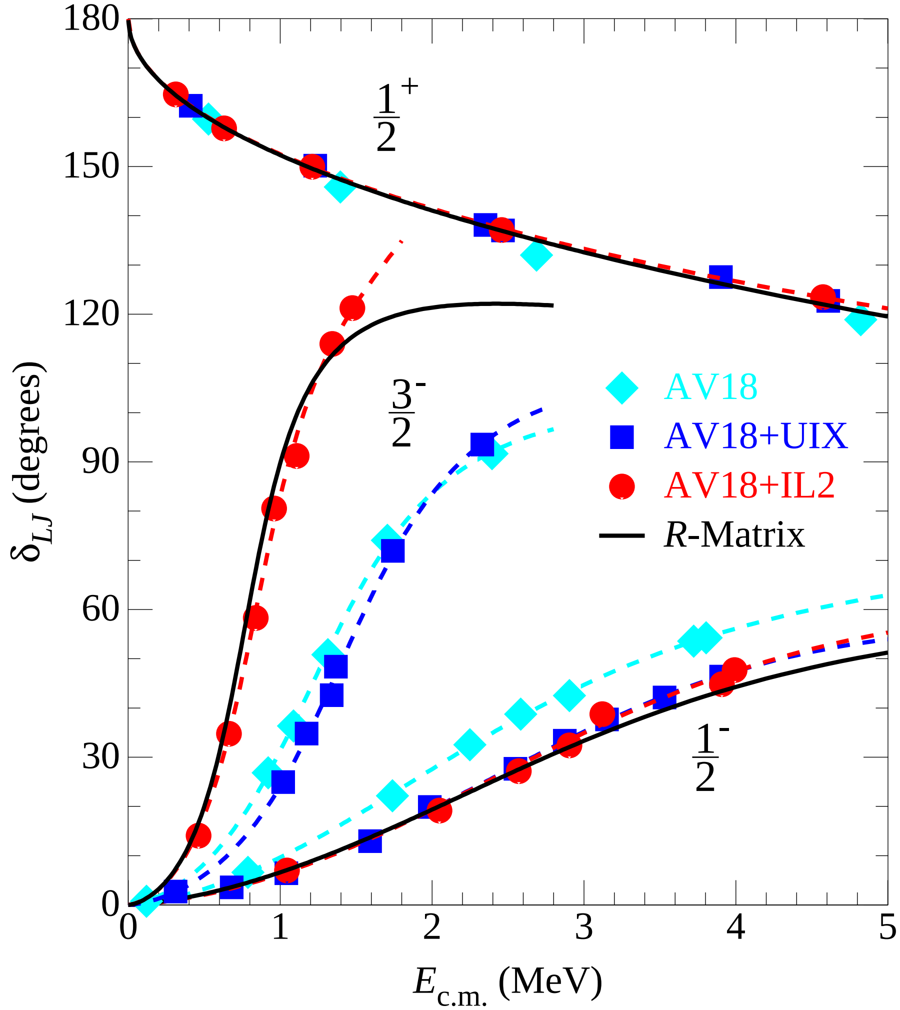

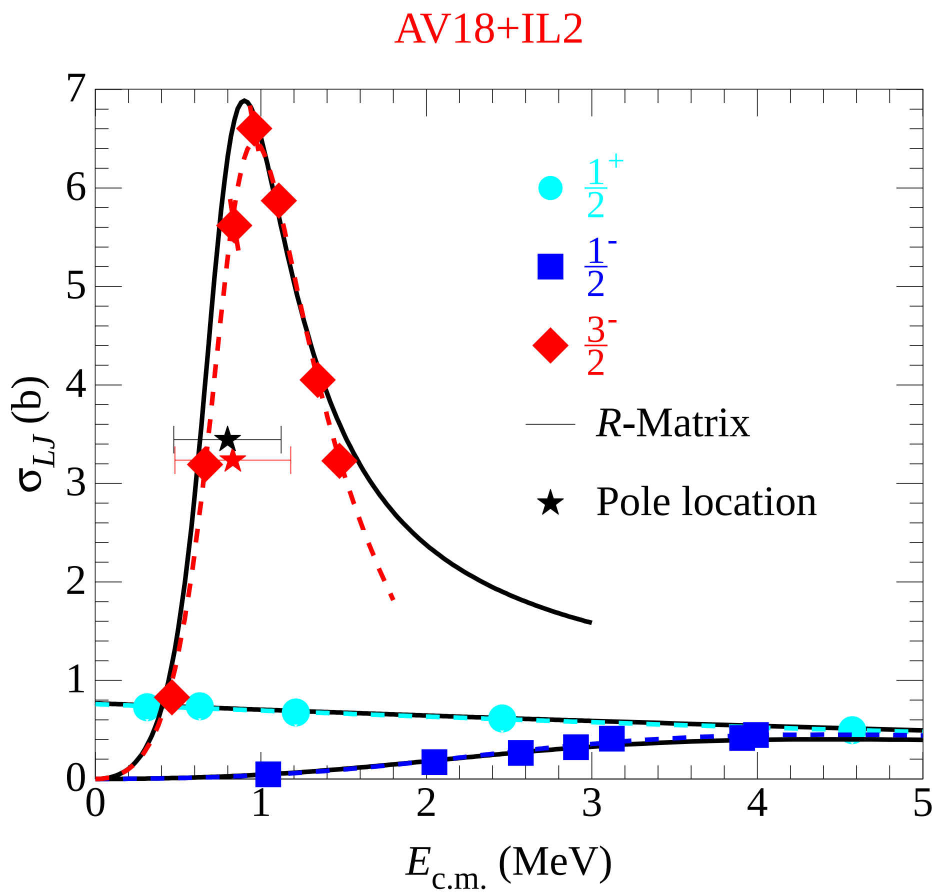

Nollett, *et al.*, PRL **99**, 022502 (2007)

Radiative Capture Reactions

$$\sigma(E_{cm}) = \frac{8\pi}{3}\frac{\alpha}{v_{\rm rel}}\frac{q}{1+q/m_{\rm Li}}\sum_{LSJ\ell}\left[\left|E_\ell^{LSJ}(q)\right|^2 + \left|M_\ell^{LSJ}(q)\right|^2\right]$$

^{3}H$(\alpha,\gamma)^7$Li ^{3}He$(\alpha,\gamma)^7$Be

Sources of ^{7}Li in big bang

^{7}Be key to solar ν_e production

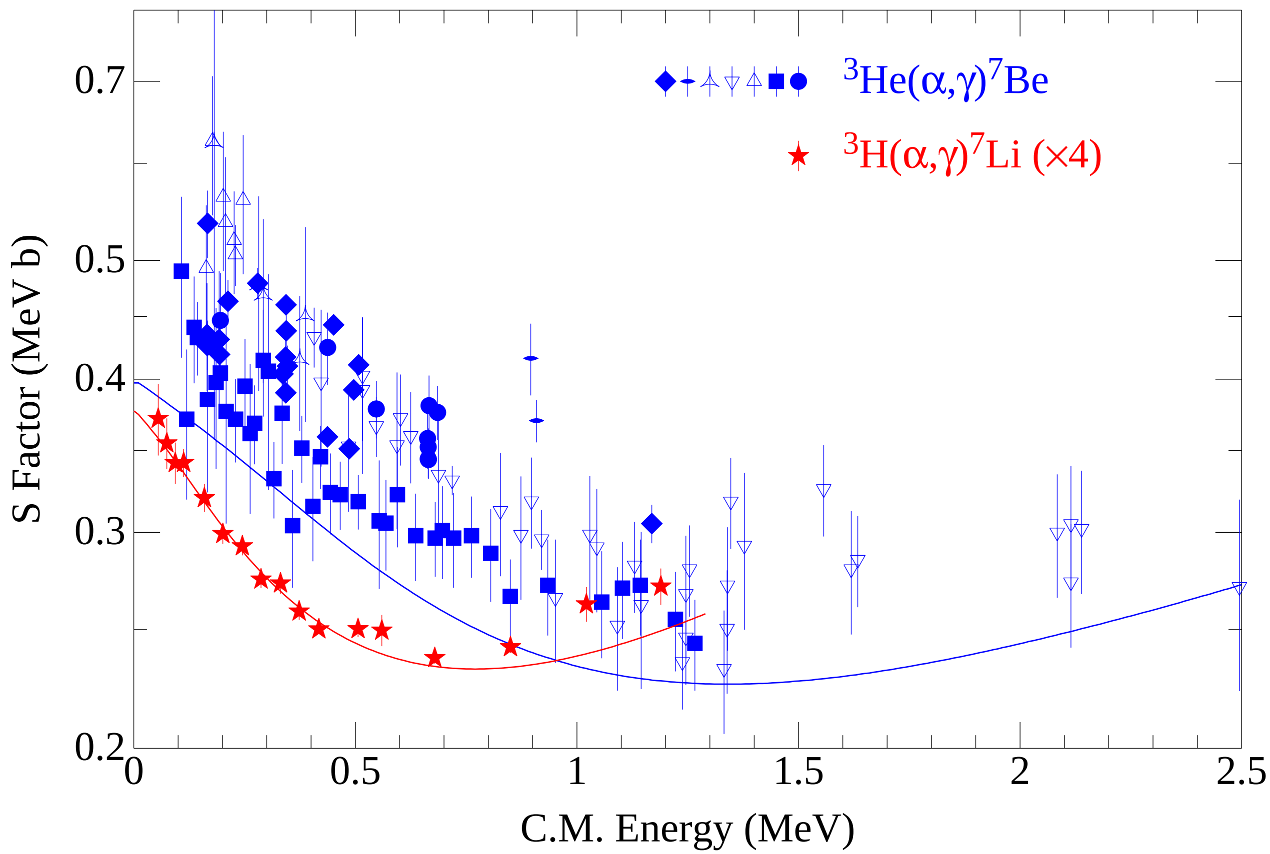

Nollett, PRC **63**, 054002 (2001)

Single-nucleon momentum distributions

$$\rho_{\sigma\tau}(k) = \int d\mathbf{r}'_1\, d\mathbf{r}_1\, d\mathbf{r}_2 \cdots d\mathbf{r}_A\, \psi^\dagger_{JM_J}(\mathbf{r}'_1, \mathbf{r}_2, \ldots, \mathbf{r}_A)\, e^{-i\mathbf{k}\cdot(\mathbf{r}_1 - \mathbf{r}'_1)}\, P_{\sigma\tau}(1)\, \psi_{JM_J}(\mathbf{r}_1, \mathbf{r}_2, \ldots, \mathbf{r}_A)$$

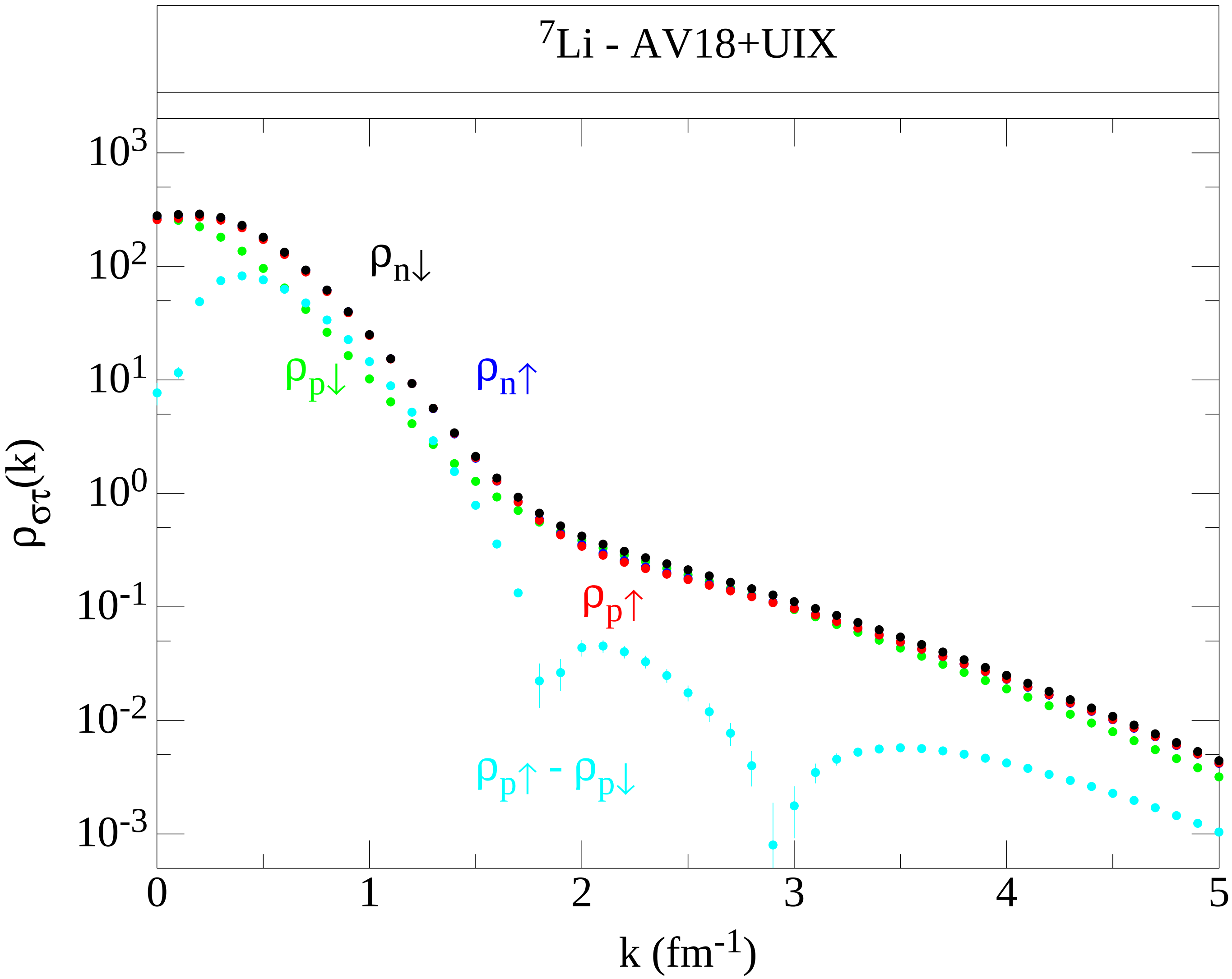

Two-nucleon & cluster-cluster distributions

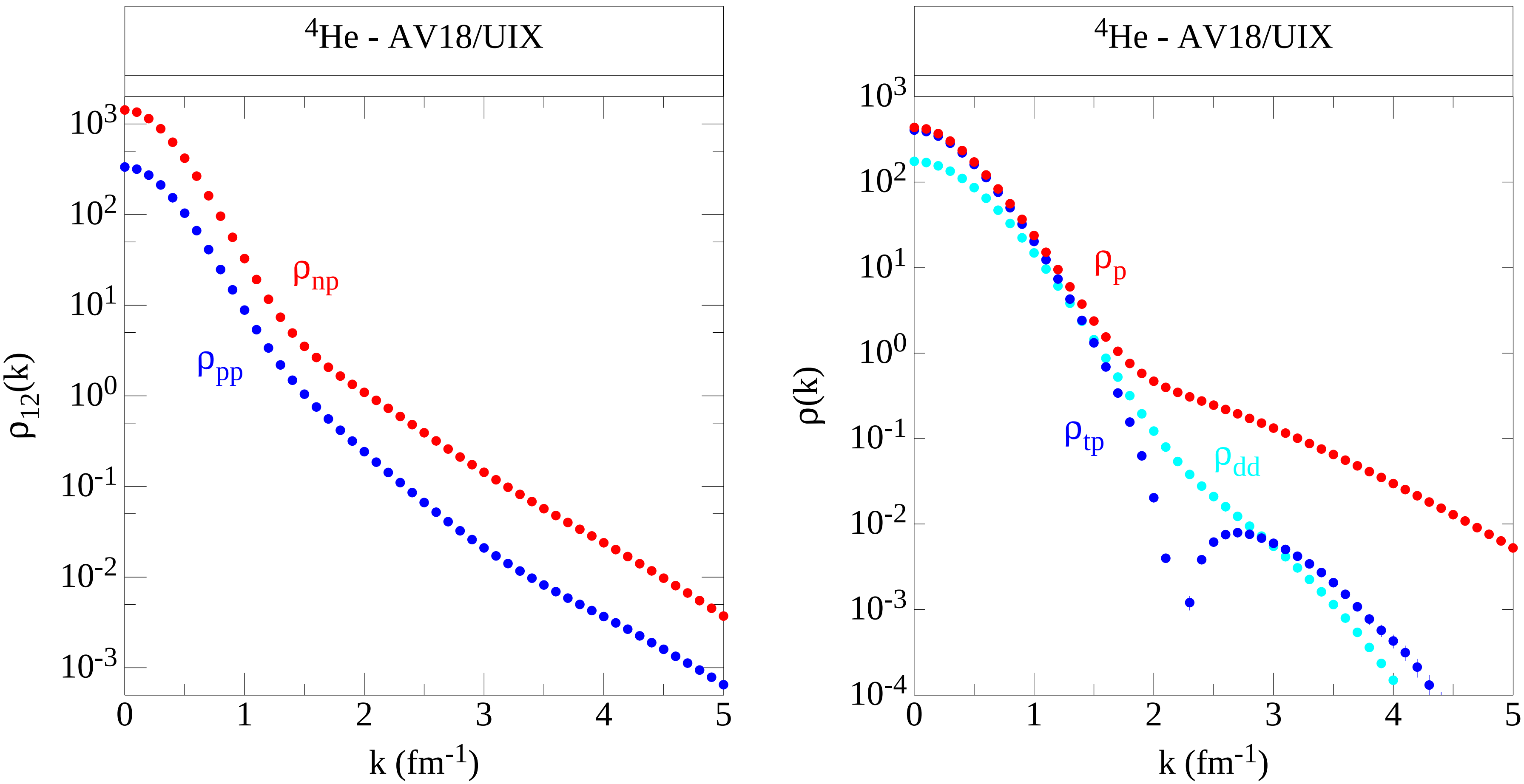

Two-nucleon Knockout – $A(e, e'pN)$

JLAB experiment for ^{12}C$(e, e'pN)$ measured back-to-back pp and np pairs

Pairs with $q_{\rm rel}$ = 2–3 fm^{-1} show np/pp ratio ≈ 10–20 Subedi *et al.*, Science **320**, 1476 (2008)

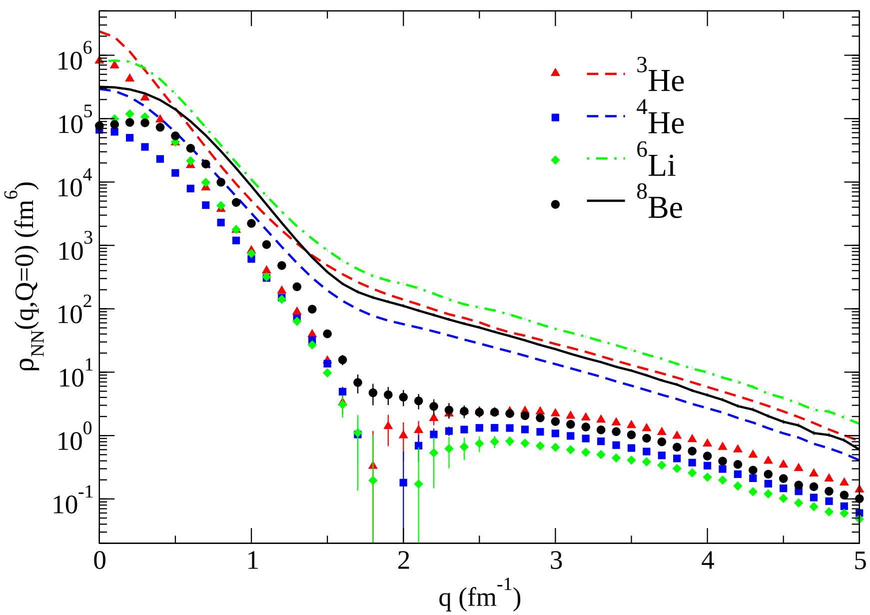

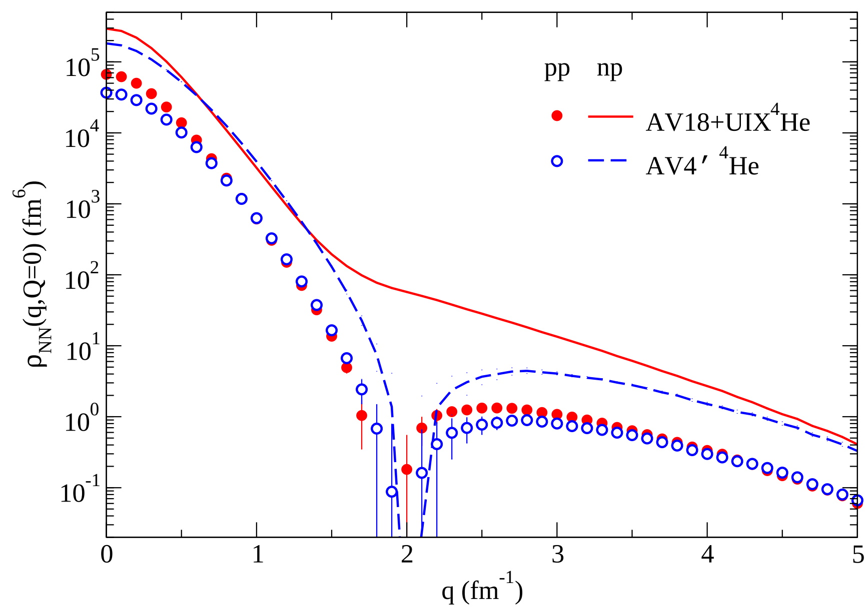

VMC calculations for pairs with $Q_{\rm tot}$ = 0 show this effect in A=3–8 nuclei

Effect disappears when tensor correlations are turned off

Shows importance of tensor correlations to > 3 fm^{-1}

Schiavilla, Wiringa, Pieper & Carlson, PRL **98**, 132501 (2007)

For $Q_{\rm tot} > 0$ $(Q \parallel q)$, the minimum in pp distribution fills in:

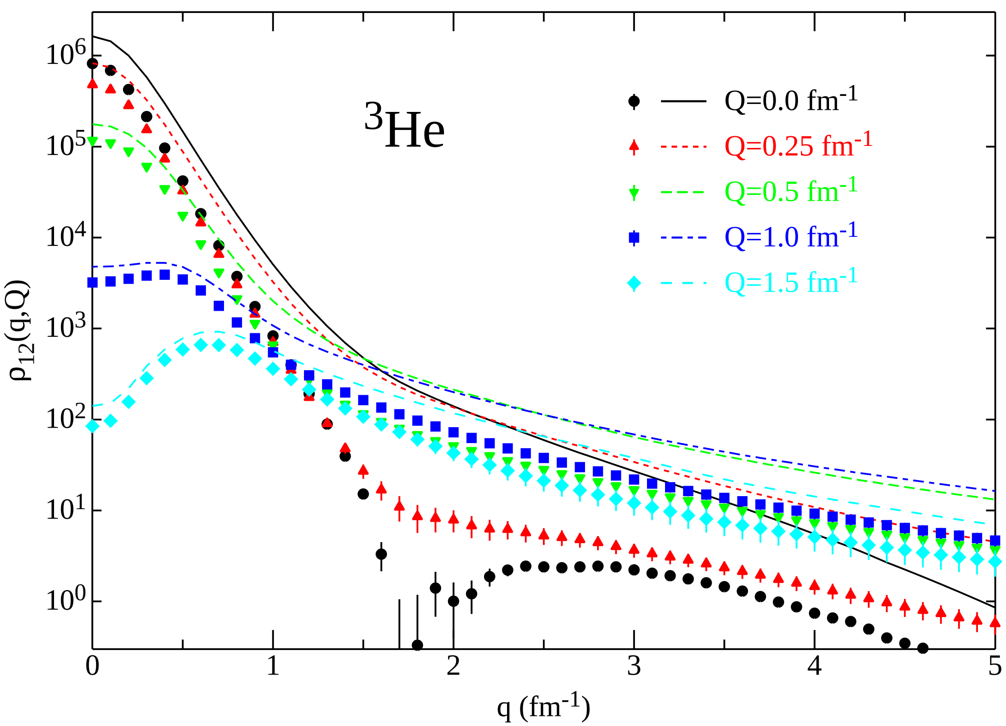

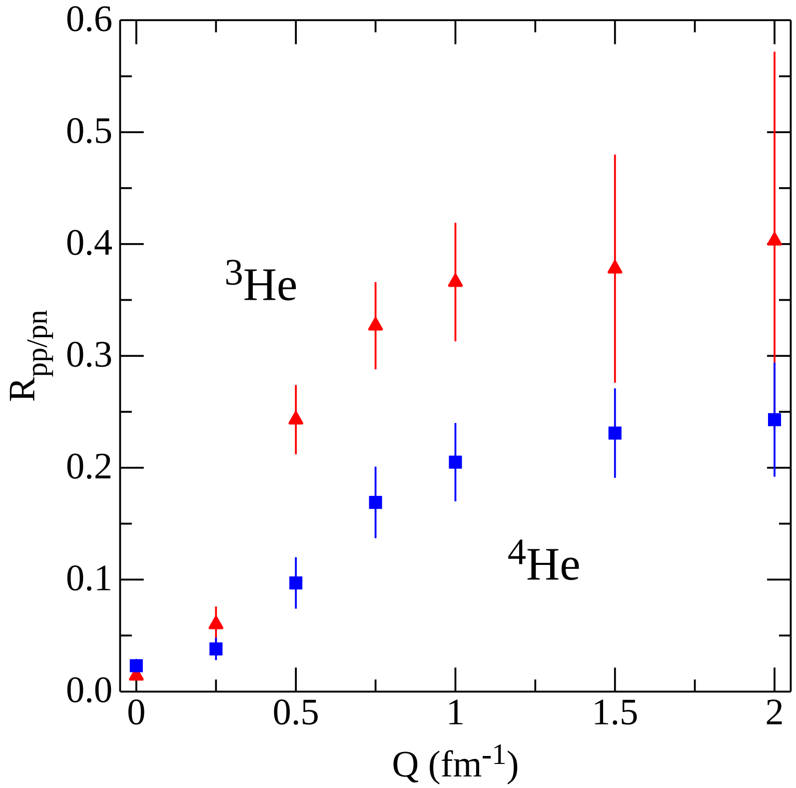

For $q_{\rm rel}$ integrated over 300–500 MeV/c, the ratio of pp to pn pairs $R_{pp/pn}$ compares well with preliminary analysis of CLAS data for ^{3}He$(e,e'pp)n$

Wiringa, Schiavilla, Pieper & Carlson, PRC **78**, 021001 (2008)

DOES IT REALLY HAVE TO BE THAT COMPLICATED?

We have excellent description of light nuclei using accurate NN potential supplemented by realistic $3N$ potential. But what happens to nuclear spectra with simpler force models?

AV8$'$: $[1,\ \sigma_i \cdot \sigma_j,\ S_{ij},\ \mathbf{L}\cdot\mathbf{S}] \otimes [1,\ \tau_i \cdot \tau_j]$

Fits CI S- and P-wave scattering data and ^{2}H

AV6$'$: $[1,\ \sigma_i \cdot \sigma_j,\ S_{ij}] \otimes [1,\ \tau_i \cdot \tau_j]$

Drop spin-orbit force - ^{3}P-wave data goes bad

readjusted to keep ^{2}H binding correct

AV4$'$: $[1,\ \sigma_i \cdot \sigma_j] \otimes [1,\ \tau_i \cdot \tau_j]$

Drop tensor force - ^{3}P-wave worse; no Q in ^{2}H

readjusted to keep ^{2}H binding correct

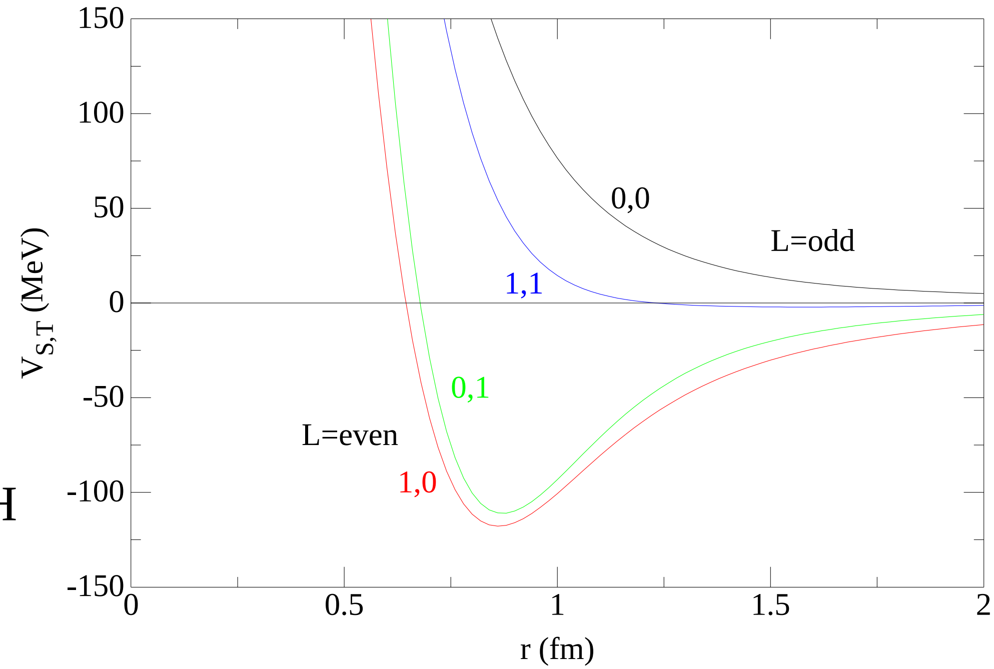

AV1$'$: $[1]$

Average L=even potential only; still has attractive well & repulsive core

both dineutron and ^{2}H weakly bound

Coulomb potential $V_C = \frac{e^2}{r}$ added between all pp pairs.

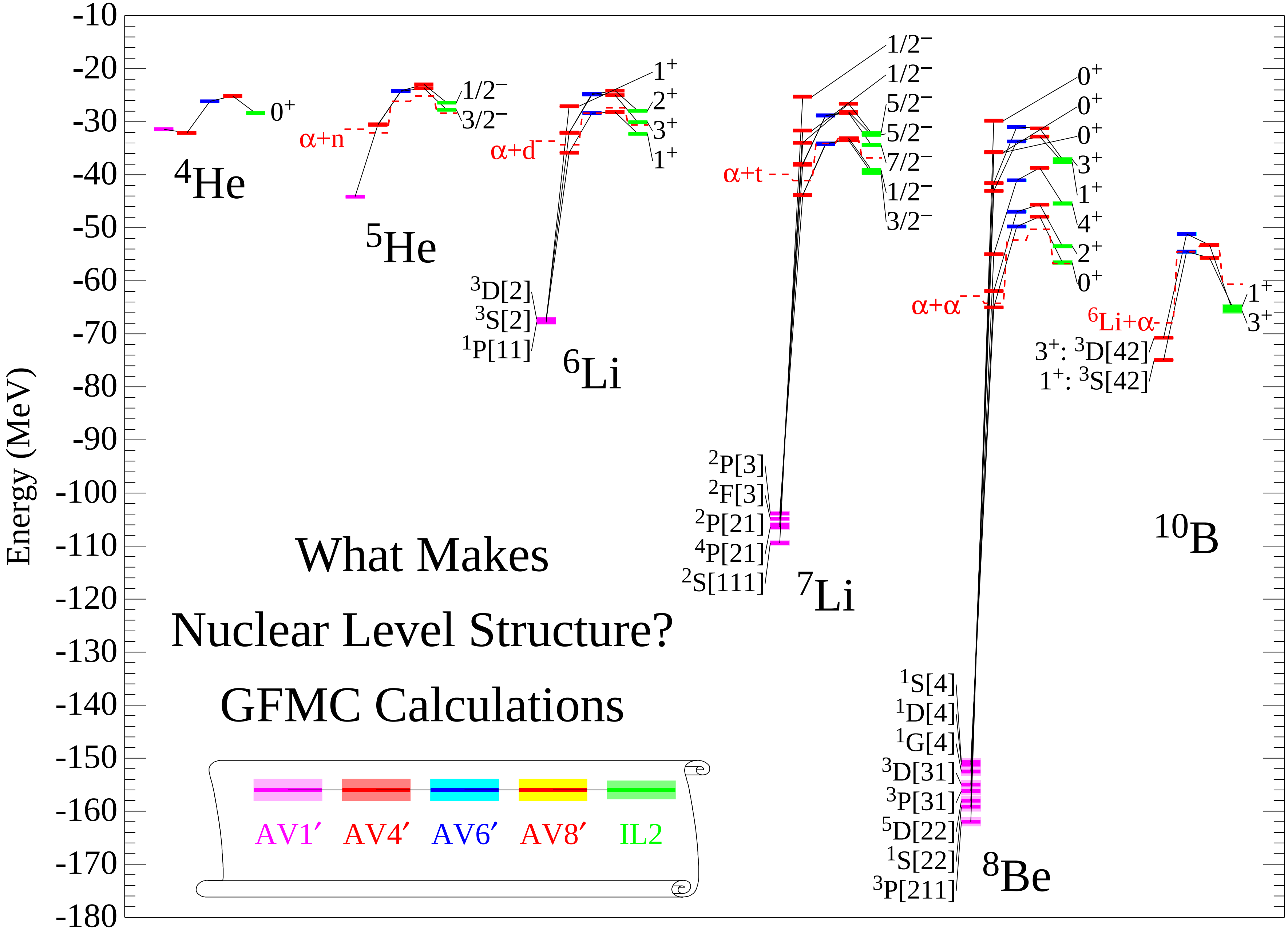

Wiringa & Pieper, PRL **89**, 182501 (2002)

Consequences

AV1$'$: approximately reproduces A=2-4 nuclear binding, but no saturation for $A > 5$. Nuclear matter $E(\rho_0)/A \approx -80$ MeV indicates repulsive core is not source of nuclear saturation. Ordering of excited states inverted and compressed compared to experiment. Big Bang would produce very heavy neutron-rich nuclei — mini-neutron stars!

AV4$'$: Much better saturation; ordering of excited states improved with less compression; A=5 no longer stable, but A=8 still stable. Indicates importance of spin-isospin exchange forces for achieving saturation.

AV6$'$: Addition of tensor force makes A=8 unstable, but stability of intervening A=6,7 nuclei too close to call.

AV8$'$: Addition of spin-orbit force definitely stabilizes ^{6,7}Li nuclei while keeping A=5 & 8 unstable; excitation spectrum looks pretty good.

This model might produce a universe much like ours!
Borromean nuclei ^{6,8}He, ^{9}Be may need V_{ijk} for stability.

Nuclear Binding and Hadronic Mass Variation

Could fundamental "constants" have varied over the history of the universe?

Theories unifying gravity with other interactions suggest the possibility of temporal and spatial variations of physical "constants" in the expanding universe.

Some evidence for variations in the fine structure constant α, strength of the strong interaction, and particle masses has been inferred from studies of big bang nucleosynthesis, quasar absorption spectra, and the Oklo natural nuclear reactor.

Program for studying the universe's dependence on the quark mass $X_q = m_q/\Lambda_{QCD}$:

- Study how hadron masses depend on quark masses
- Evaluate how nuclear binding depends on hadron masses
- Study consequences for big bang and stellar nucleosynthesis

Hadron mass dependence on current-quark mass

Prediction from a Dyson-Schwinger equation study of the sigma terms of light-quark hadrons:
V.V.Flambaum, A.Höll, P.Jaikumar, C.D.Roberts and S.V.Wright [FBS **38**, 31 (2006)]

$$\frac{\delta m_H}{m_H} = \frac{\sigma_H}{m_H} \frac{\delta m_q}{m_q} \qquad m_q = (m_u + m_d)/2$$

	π	ρ	ω	N	Δ
$\frac{\sigma_H}{m_H}$	0.498	0.021	0.034	0.064	0.041

Other models are possible, but we expect pion mass to vary most rapidly due to Gell-Mann-Oakes-Renner relation $m_\pi^2 = m_q$ and that other masses will vary in the same direction, i.e., all get larger or smaller together.

HAMILTONIAN DEPENDENCE ON HADRON MASS

Consider Hamiltonian with three different interaction models:

- Argonne v_{28} (AV28) : coupled-channels OPE with explicit Δ's fit to 1981 phase shifts
- Argonne v_{14} (AV14) : nucleons-only with approximate TPE, phase-equivalent to AV28
- Argonne v_{18} (AV18) : updated AV14 with charge-independence-breaking fit to 1993 data, weaker $f_{\pi NN}$, deeper well, stiffer core; supplement with Urbana IX (UIX) V_{ijk}

and allow m_N, m_Δ, m_π, and $m_V\,[= \frac{1}{2}(m_\rho + m_\omega)]$ to vary.

m_N (m_Δ) enters explicitly through kinetic energy K_i and implicitly through 2π-exchange v^I_{ij}
m_π enters explicitly through v^π_{ij} ($V^{2\pi P}_{ijk}$) and implicitly through 2π-exchange v^I_{ij}
m_V enters implicitly through short-range v^S_{ij}

Evaluating mass dependence

Change hadron masses m_H one at a time $\pm 0.1\%$ and recalculate E. Two-nucleon cases evaluated exaclty. Multi-nucleon cases evaluated using variational Monte Carlo.

Results can be expressed as dimensionless derivatives:

$$\Delta\mathcal{E}(m_H) = \frac{\delta E/E}{\delta m_H/m_H}$$

and combined with given model (such as DSE) for correlation between hadron and quark masses:

$$E(m_q) = E_0 \left[1 + \sum_{m_H} \Delta\mathcal{E}(m_H) \frac{\delta m_H(m_q)}{m_H} \right]$$

Two-nucleon binding energy dependence on quark mass from DSE studies

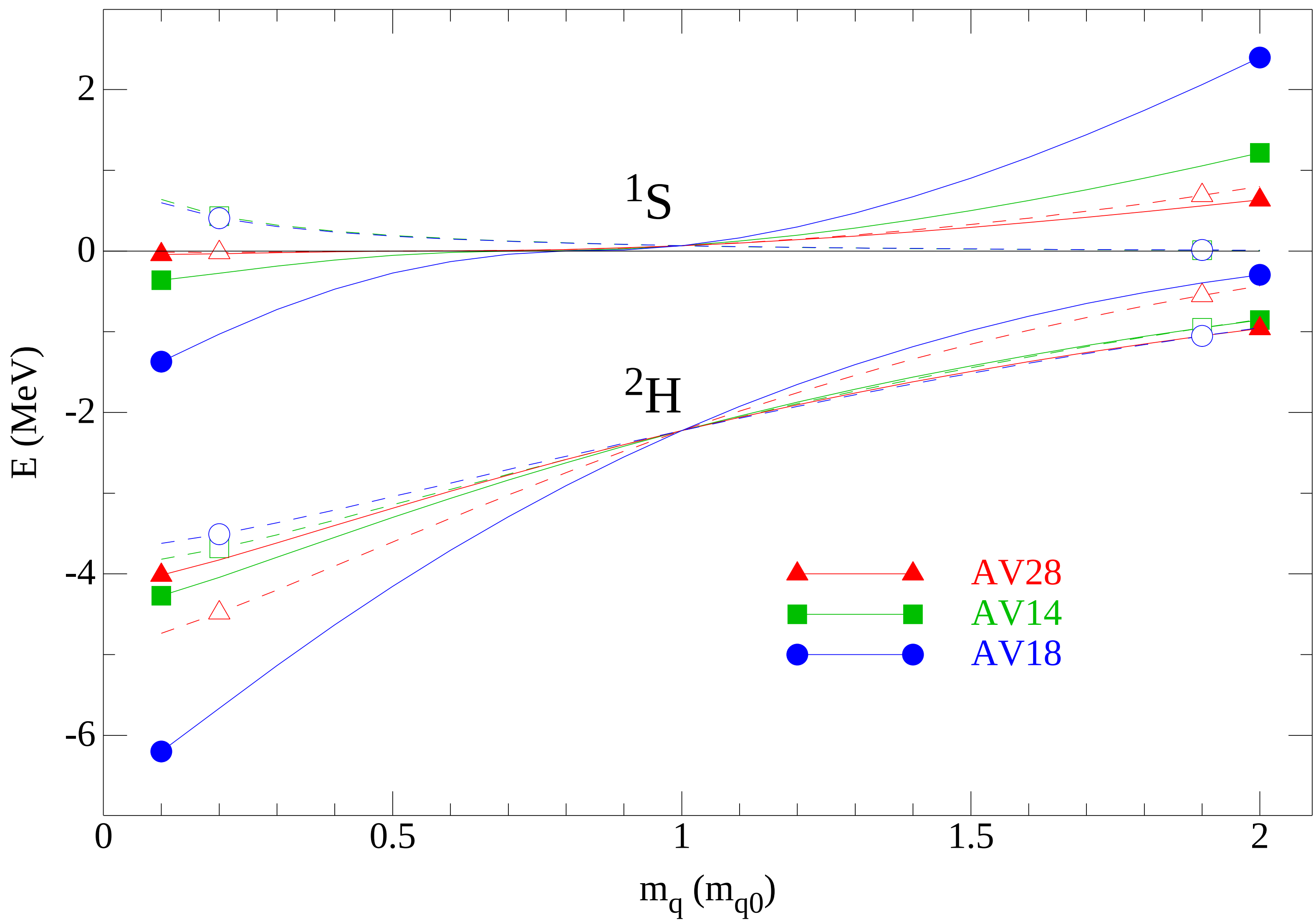

Multi-nucleon $E(m_q)$ for "full" AV18+UIX calculation with DSE $\delta m_H / m_H$

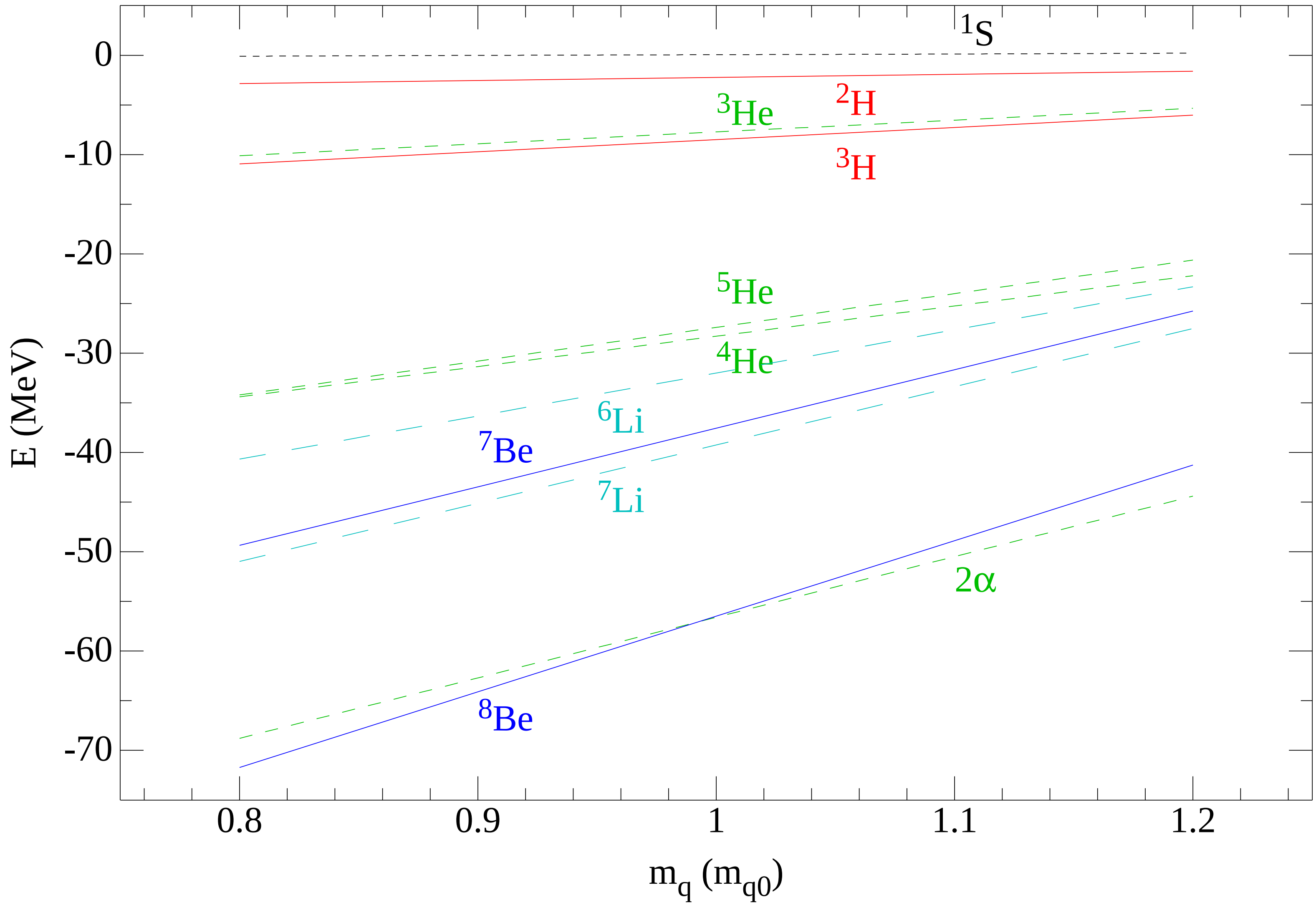

CONSEQUENCES FOR BIG BANG

Dent, Stern, and Wetterich, [PRD **76**, 063513 (2007)] calculated sensitivity of BBN abundances for ^{2}H, ^{4}He, and ^{7}Li to variations in A=2-7 binding energies. Folding our results with theirs, we find these BBN abundances will be in much better agreement with the WMAP value of η (baryon to photon ratio) for $\delta X_q/X_q = K \cdot (0.013 \pm 0.02)$ where $K = \frac{\delta E/E}{\delta m_q/m_q} \sim 1$ is the total sensitivity to the light quark mass.

K	$^1S_0(np)$	^{2}H	^{3}H	^{3}He	^{4}He	^{5}He	^{6}Li	^{7}Li	^{7}Be	^{8}Be
AV28	4.5	-0.75								
AV14	7.3	-0.84	-0.89	-0.96	-0.69	-0.81	-0.89	-1.03	-1.09	-0.92
AV18+UIX	11.4	-1.39	-1.44	-1.55	-1.08	-1.24	-1.36	-1.50	-1.57	-1.35

Flambaum & Wiringa, PRC **76**, 054002 (2007)

Flambaum & Wiringa, PRC **79**, 034302 (2009)